

THESIS APPROVAL

The abstract and thesis of Donald Nichols Lindsay for the Master of Science in Geology presented July 16, 2003, and accepted by the thesis committee and the department.

COMMITTEE APPROVALS:

Andrew G. Fountain, Chair

Joseph S. Walder

Scott F. Burns

Trevor D. Smith
Representative of the Office of Graduate Studies

DEPARTMENTAL APPROVAL:

Micheal C. Cummings, Chair
Department of Geology

ABSTRACT

An abstract of the thesis of Donald Nichols Lindsay for the Master of Science in Geology presented July 16, 2003.

Title: Englacial Hydrology Related to an Outburst Flood from Hidden Creek Lake, a Glacially-dammed Lake in Alaska.

The primary focus of this research project was to take advantage of a lake having a history of annual outburst floods to study the mechanisms responsible for the subglacial release of glacially-impounded lake waters. The site is Hidden Creek Lake, which is dammed by the Kennicott Glacier, in the Wrangell-St. Elias National Park, Alaska. This research project consisted of three subsidiary studies. First, a hydrologic model was constructed to estimate historic lake volumes to determine whether the time of outbreak correlates with changes in lake stage and meteorological factors. In addition, by evaluating the location of the snowline, the model was used to estimate the location of the "fast" hydraulic system to determine if a correlation exists between it and the time of outbreak. Second, water level data obtained from a borehole drilled into the glacier was analyzed to investigate how the englacial hydrology reacted in response to lake level drop during the flood. Lastly, the flood discharge was modeled mathematically to determine if any insight into the physical processes governing flood initiation could be gained. Results obtained from the use of the hydrologic model indicate that there does

not appear to be any correlation between lake level and the time of outbreak, a declining trend in peak lake level could be the result of a reduction of the ice dam thickness, and the location of the snowline appears to correlate with the time of outbreak, may provide a key role in predicting the release of future outburst floods. Borehole water level observations indicate the lake and englacial hydraulic systems fluctuate congruently after a connection between the two was made. Lastly, it is speculated that constrictions occurring within the englacial hydraulic system as the lake drained resulted in the measured flood hydrograph deviating from the idealized, mathematically modeled flood hydrograph.

ENGLACIAL HYDROLOGY RELATED TO AN OUTBURST FLOOD FROM
HIDDEN CREEK LAKE, A GLACIALLY-DAMMED LAKE IN ALASKA

by

DONALD NICHOLS LINDSAY

A thesis submitted in partial fulfillment of the
requirements for the degree of

MASTER OF SCIENCE
in
GEOLOGY

Portland State University
2003

ACKNOWLEDGMENTS

First and foremost, I would like to thank my advisor, Dr. Andrew Fountain, for providing me with such a wonderful and rewarding research experience: you got me studying things I thought I would never study and seeing places I thought I would never see. Without your support, patients, upbeat attitude, and welcomed editorial comments, this thesis would not be a reality.

I would like to thank Dr. Joe Walder for his help with the numerical modeling portion of the thesis, his review and welcomed comments pertaining to many of my ideas along the way, and his unique and enjoyable sense of humor while spending time with him in the field.

In addition to Andrew and Joe, I would also like to thank the other members of my committee, Dr. Scott Burns and Dr. Trevor Smith, for their review of this manuscript and the knowledge they passed on to me in the fields of engineering geology and geotechnical engineering, respectively.

A special thanks needs to be given to my field and research mates Robert Schlicting, Michelle Cunico, and Dennis Trabant. I appreciate the help you gave me throughout the development of my thesis, and the camaraderie we established will stay with me for a lifetime.

I would like to thank my brother, Will, who opened his house up to Cindy and I while I was pursuing my masters degree.

Last, but far from least, I owe a great deal of gratitude to my wife, Cindy, who has provided love and support throughout the years. Without your encouragement, patience, and selfless sacrifices, this project would not have been possible. Thank you, Cindy.

TABLE OF CONTENTS

ACKNOWLEDGMENTS	i
LIST OF TABLES	v
LIST OF FIGURES	vi
CHAPTER 1 – INTRODUCTION AND PROJECT DESCRIPTION.....	1
Introduction	1
Objectives.....	4
Study Area.....	5
Geology.....	7
CHAPTER 2 - BACKGROUND	9
General overview on ice-dammed outburst floods	9
Glacial hydrology.....	10
Release Mechanism	15
Past work related to the Study Area	17
CHAPTER 3 – SNOW ACCUMULATION AND RUNOFF MODEL	20
Introduction	20
Correlating outbreak timing to meteorological variables	21
Hydrologic Model	25
Model Overview	25
Calculating Precipitation at Elevation.....	26
Calculating Temperature at Elevation.....	28
Calculating Snowmelt.....	29
Testing the Runoff Model	32
Application to Hidden Creek Lake.....	38
Analyses	43
Testing the Flotation and Cantilever Mechanisms	43
Location of the subglacial hydraulic system.....	47
Summary	49
CHAPTER 4 - BOREHOLE WATER LEVEL ANALYSIS	51
Introduction	51
Field Program and Methods	52
Chronology of events	55
Results	59
Interpretation	62
Summary and Discussion	66

CHAPTER 5 – MODELING THE OUTFLOW HYDROGRAPH.....	68
Introduction	68
Comparison Data.....	68
Walder and Costa Model	70
Clarke Model.....	72
Results	77
Lake Volume.....	80
Length of Drainage System.....	82
Roughness of the Drainage System.....	83
Initial Ice Thickness and Lake Elevation above Seal	83
Combination of Physical Parameters	84
Speculation on Physical Obstructions.....	85
CHAPTER 6 – DISCUSSION AND CONCLUSIONS.....	88
Summary	88
Suggestions for future research	90
REFERENCES CITED.....	93

LIST OF TABLES

Number	Page
Table 1: Correlation of date of outbreak with cumulative degree-day index. July 1 is Julian Day 182.	23
Table 2: Correlation of date of outbreak with the total precipitation falling at hidden Creek Lake from September 1 to July 1	24
Table 3: Little Susitna River area distribution and enhancement factors	34
Table 4: Total discharge calculated using runoff model compared to the gaged volume of Little Susitna River.....	34
Table 5: Results of a sensitivity analysis performed on the input variables of the runoff model.....	37
Table 6: Hidden Creek basin area distribution and enhancement factors	39
Table 7: Measured and calculated lake volume compared	41
Table 8: Estimates of water level for 13 of the most well known flood events from Hidden Creek Lake	44
Table 9: Model inputs	73

LIST OF FIGURES

Number	Page
Figure 1: Location map of hidden Creek Lake, Kennicott Glacier, and the surrounding area.	7
Figure 2: Diagram showing the profile and cross-section view of R-channels beneath glaciers	12
Figure 3: Schematic showing the profile (A) and cross-section view (B) of a linked-cavity system (Adapted from Kamb, 1987).....	14
Figure 4: Plot of degree-day sum against the day of outbreak.	23
Figure 5: Plot of cumulative precipitation to date of outbreak	24
Figure 6: Flow chart of runoff model.	27
Figure 7: Plot of precipitation with increasing altitude up the Kennicott Glacier Valley. Data obtained from PRISM.....	28
Figure 8: Illustration showing the location and extent of the Little Susitna River basin	35
Figure 9: Plot of modeled discharge volumes compared to measured discharge volumes for 10 water years on the Little Susitna River. The line fit to the results is through the origin and the error bars indicate $\pm 21\%$ error.....	36
Figure 10: Area verses altitude (hypsoetry) distribution of Hidden Creek Lake.	40
Figure 11: Volume verses altitude distribution of Hidden Creek Lake.....	40
Figure 12: Comparison of estimated lake volumes against modeled lake volumes ...	41

Figure 13: Comparing estimated volumes to correlated modeled volumes	43
Figure 14: Plot of calculated lake level against time of outbreak for Hidden Creek Lake	46
Figure 15: Plot comparing the location of the snowline to the time of outbreak	49
Figure 16: Aerial photo showing the location of the drill site (star) in relation to the lake (top of photo). Fore scale, the width of the ice dam is approximately 1 km wide. The top of the photo is to the west.	53
Figure 17: Diagram of borehole depicting the observations made during drill operations	56
Figure 18: Photo showing fresh fractures that propagated through the drill site. The width of the fractures are approximately 4-7 cm wide.	58
Figure 19: Fractures (arrows) observed within drained borehole on July 20, 1999. The photo is looking vertically down the borehole	58
Figure 20: View of englacial conduit with sediment pouring from it. The inset provides a cross-section view of the conduit geometry. The borehole, highlighted with broken white line, is approximately 8-10 cm wide.	59
Figure 21: A) Plot of air temperature and borehole water level. B) Plot of lake and borehole water elevations	61
Figure 22: Illustrated plot of air temperature, and borehole and lake water elevations	63
Figure 23: Illustrated plot showing the slope of portions of the borehole record	64
Figure 24: Plot comparing borehole and lake water elevations as the lake drained ...	66

Figure 25: Plot of the flood hydrograph exiting Hidden Creek Lake. Assuming a vertical falling limb (dashed line) after the lake dropped below instrumented elevation 69

Figure 26: Plot showing the relation of lake volume to peak discharge, after Walder and Costa (1996). The black triangle is the 1999 HCL flood and the gray diamonds are floods from the Walder and Costa (1996) dataset 71

Figure 27: Predicted hydrographs using Clarke’s 1982 solution. The point at which the graphs terminates is when the volume within the lake goes to zero 79

Figure 28: Plot comparing the modeled and measured hydrographs 79

Figure 29: Comparison of modeled versus measured hydrographs where the lake temperature is held constant at 1 degree Celsius and lake volume varied by 20% 81

Figure 30: Plot comparing the measured hydrograph to modeled hydrographs with varying lengths and roughness 82

Figure 31: Plot comparing the measured hydrographs with the best combination of parameters where V_o is $16.5 \times 10^6 \text{ m}^3$, θ is 3°C , l_o is 16,000 m, n' is 0.1, and h_i is 481 m 85

CHAPTER 1 – INTRODUCTION AND PROJECT DESCRIPTION

Introduction

Glacial outburst floods, or jökulhlaups, may be broadly defined as the sudden release of water stored either within a glacier or dammed by a glacier (Fountain and Walder, 1998). Outburst floods have been reported in all glacierized regions of the world and may be triggered by a) the sudden drainage of an ice-dammed lake below or through an ice dam; b) lake water overflow and rapid fluvial incision of ice, bedrock or sediment barriers; or c) the growth and collapse of subsurface reservoirs (Benn and Evans, 1998).

Due to their rapid and high discharge, outburst floods have devastating effects downstream; they pose a threat to human life and infrastructure, and cause river channel instability and channel migration (Rickman and Rosenkrans, 1997). The largest known outburst floods within the continental United States occurred over 12,000 years ago and came from Glacial Lake Missoula, a large ice-dammed lake formed by the Pleistocene Cordilleran Ice Sheet. Known as the Missoula Floods, these outburst floods may have reached peak discharges of roughly $21 \times 10^6 \text{ m}^3 \text{ s}^{-1}$. The erosive nature of these immense floods created what is referred to today as the Channeled Scablands of Southeastern Washington (Waitt, 1980; O'Connor and Baker, 1992). Although the Missoula Floods occurred some time ago, under climatic conditions that no longer persist, outburst floods remain a threat in glaciated areas today. An example of this threat includes destructive debris flows caused by outburst floods that frequently move along stream valleys

positioned on the flanks of glacierized Mount Rainier, Washington (Walder and Driedger, 1995). These debris flows have repeatedly damaged facilities and road infrastructure in Mount Rainier National Park (Walder and Driedger, 1995).

Despite the impacts that outburst floods have had in Washington State, and in glaciated terrain located elsewhere in the world, there remains to be a number of unknowns surrounding the cause of outburst floods. Our knowledge of subglacial outburst floods, both practical and theoretical, is largely derived from the study of Grimsvötn (a subglacial ice-dammed lake) on the Vatnajökull ice cap, Iceland. The celebrated Grimsvötn outbursts are the product of subglacially released water that is derived primarily from volcanic heat that melts the bottom of the ice cap. On average, the Grimsvötn outbursts release about 4.5 km^3 of water at a peak discharge of about $50,000 \text{ m}^3 \text{ s}^{-1}$ (Nye, 1973; Björnsson, 1974). Based on studies of Grimsvötn outbursts, Thöranson (1939), Björnsson (1974), and Nye (1976) developed some of the earliest hypotheses and models for the rapid release of water through glaciers. Despite their efforts, however, and the efforts of scientists that have followed them, a clear mechanism of drainage initiation remains elusive. This elusiveness in drainage initiation is likely the result of uncertainties in the factors that control the subaerial release of outburst floods. Some of these factors include the rate of water flowing into the lake, lake topography, effectiveness of the ice dam to impound water, glacier movement, and the occurrence and role of englacial or subglacial hydraulic systems to convey the flood water (Clarke, 1982; Tweed and Russell, 1999).

Provided the factors controlling outburst initiation could be precisely analyzed, it is thought that an improved understanding of the mechanism of outburst flooding could be achieved. Moreover, it is anticipated that with this improved understanding, the impacts to human life and development caused by outburst floods could be reduced. In this regard, the purpose of this research project is to obtain a better understanding of the factors controlling the outburst of a glacier-dammed lake known as Hidden Creek Lake, located in the Wrangell –St. Elias National Park and Preserve, Alaska.

This research project was a collaborative effort involving Dr. Joseph Walder with the United States Geological Survey (USGS), Dr. Suzanne Anderson of the University of California, Santa Cruz (UCSC), and Dr. Andrew Fountain of Portland State University (PSU). The responsibility of the USGS was to measure the volume of water stored in the lake prior to release, to measure the rate of discharge exiting the lake during the release, and to monitor the deflection of the glacier in response to changing lake water elevation. UCSC monitored the stream flow at the glacier terminus to aid in modeling the flood through the glacier and to analyze the down stream geomorphic effects of the outburst flood. My responsibility was to study the subglacial hydraulic system through a network of boreholes established in the glacier to determine its role in the release of water from Hidden Creek Lake, in addition to modeling the flood from the lake to the terminus of the glacier.

Objectives

The primary objective of my research was to elucidate the mechanisms responsible for the subglacial release of glacially-impounded lake waters. By studying the drainage mechanism at Hidden Creek Lake, it is anticipated that a process-based understanding of outburst initiation is achieved that can apply to other glacier-dammed lakes. Unfortunately, we were unable to drill to the bottom of the glacier (as explained later), and we could not investigate the changing subglacial condition directly. Instead, I focused on three different but related studies. First, a hydrologic model was constructed to estimate historic lake volumes to determine whether the time of outbreak correlates with changes in lake stage and meteorological factors. If a correlation between these factors and outbreak timing is present, the results can be used to infer some of the processes controlling the flood timing. In addition, such a correlation could be used to predict future floods and reduce the hazard posed by historically unpredictable outburst floods. Second, water level data obtained from a borehole drilled into the glacier was analyzed to investigate how the englacial hydrology reacted in response to lake level drop during the flood. Lastly, the flood discharge was modeled mathematically to determine if any insight into the physical processes governing flood initiation could be gained.

In performing these three separate studies, I set out to test the following three hypotheses:

1. *The timing of outbreak correlates with factors including meteorological variables such as temperature and precipitation, changes in ice-dam thickness,*

or to the development of “fast” subglacial hydraulic systems that allow the water to drain.

2. *Valuable insight into the mechanisms that control the subglacial release of glacially impounded water can be obtained through monitoring the englacial hydraulic system through a borehole established within the ice dam.*
3. *The temporal evolution of the lake discharge conforms to established mathematical models.*

Study Area

Hidden Creek Lake (HCL) is situated at a latitude of 61°34'N and a longitude of 143°05'W on the western margin of the Kennicott Glacier, north of the town of McCarthy, Alaska (Figure 1). HCL is located approximately 16 km from the terminus of Kennicott Glacier and is the largest glacial-dammed lake in the Kennicott Glacier basin (Rickman and Rosenkrans, 1997). The primary inflow to HCL is Hidden Creek. The basin of Hidden Creek has a drainage area of 69 km², ranges in elevation from approximately 915 m to over 2,225 m above mean sea level (m.a.s.l.), and is approximately 30% glacierized. A lobe of ice from Kennicott Glacier protrudes into the mouth of Hidden Creek Basin and is referred to as the “re-entrant ice” or “ice dam”. The reported volume of water retained in the lake at the time of outbreak is approximately 10⁷ m³ (Rickman and Rosenkrans, 1997).

Since 1911, the lake has drained annually, within a two-day period, in mid- to late summer. The timing of outbreak has been recorded based on direct observation or

anecdotal evidence from residences of the town of McCarthy and those people affiliated with Kennecott mine, a large, non-operational copper mine located approximately 5 miles north of McCarthy on the east side of Kennicott Glacier (Rickman and Rosenkrans, 1997).

In addition to HCL, several smaller glacial-dammed lakes are located within the Kennicott Glacier basin. These lakes include Jumbo Lake, Donoho Lake and Erie Lake located on the eastern flank of Kennicott Glacier (Figure 1). Although all the lakes are known to drain, Jumbo and Donoho Lakes generally drain prior to HCL, then partially refill with turbid water while HCL drains (Rickman and Rosenkrans, 1997). Once HCL stops draining, the turbid water within Jumbo and Donoho lakes begins to drain (Rickman and Rosenkrans, 1997).

HCL was chosen for this study primarily for its history of outburst floods and extensive historic record of lake level observations since the early 1900s. In addition, HCL makes a good candidate because of the access to both the lake and the terminus of Kennicott Glacier and the presence of a permanent footbridge that crosses the Kennicott River, providing a stable platform to measure stream flow from the glacier.

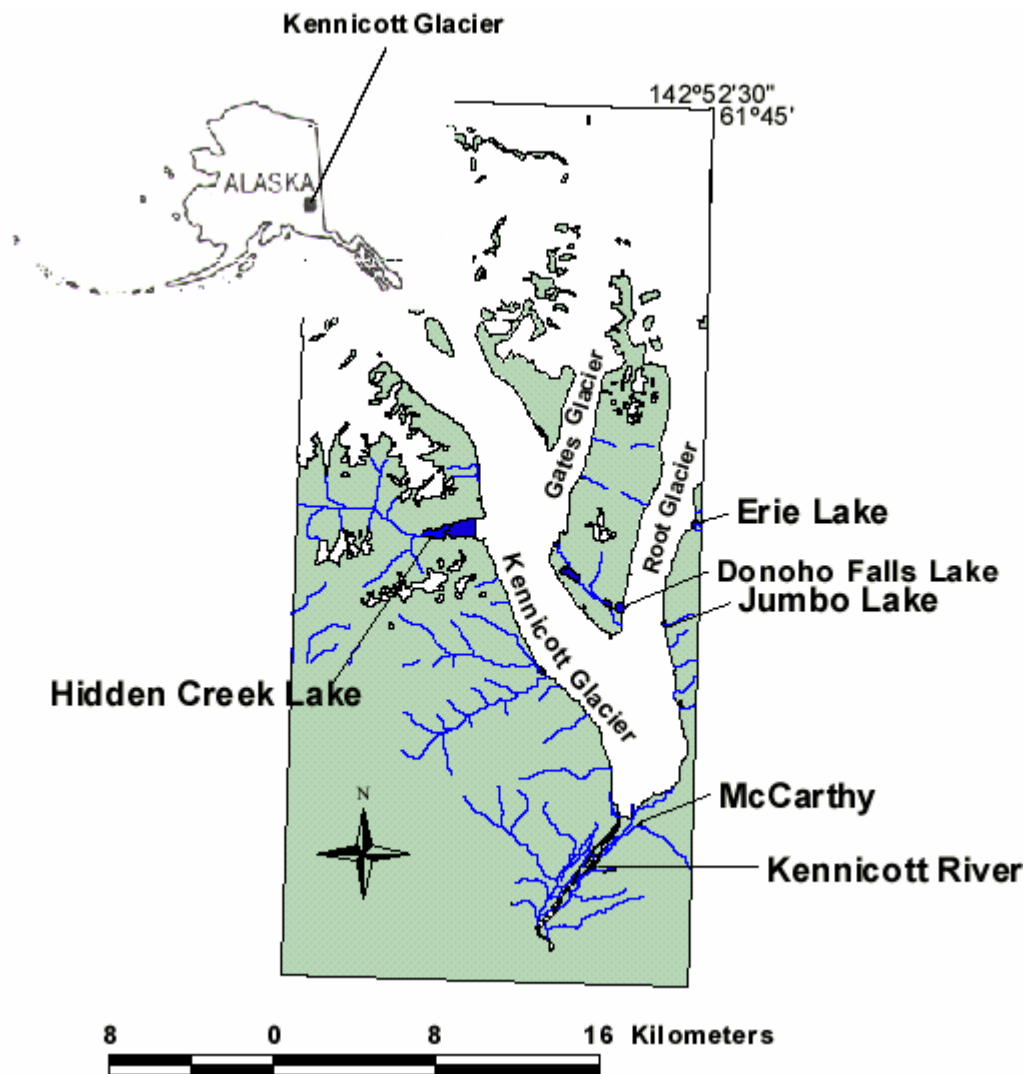


Figure 1. Location map of Hidden Creek Lake, Kennicott Glacier, and the surrounding area.

Geology

The upper basin of Kennicott Glacier resides on the southeastern flank of Mount Blackburn. Mount Blackburn rises about 4,998 m a.s.l., and is the erosional remnant of a large volcano. It is the oldest volcano out of several that are collectively referred to as

the Wrangell volcanic field (Richter et al., 1995). The Wrangell volcanic field formed as a volcanic back arc about 26 million years ago, when the Yakutat terrane began to subduct beneath the continental North American plate (Richter, et al., 1995). The composition of the Wrangell volcanic field includes subaerial andesitic lava flows, pyroclastic rocks, and intrusions of felsic hypabyssal rock, all of which are Tertiary in age (MacKevett, 1972). At the confluence with the Gates Glacier (Figure 1), the Kennicott Glacier crosses an unconformity. This unconformity separates the younger rock of the Wrangell volcanic field from older rock of the Root Glacier Formation. The Root Glacier Formation is upper Jurassic in age and includes sedimentary sandstones, siltstones, shales, and conglomerates (MacKevett, 1972). From the Gates Glacier down to the terminus of Kennicott Glacier, the bedrock is made up of predominately the Chitistone Limestone, Nizina Limestone, Nikolai Greenstone, all of Triassic age, and of the McCarthy Formation of Triassic and Jurassic age (MacKevett, 1972). Exposed within Hidden Creek Valley are the Nikolai Greenstone and the Chitistone and Nizina Limestones.

Structurally, the Kennicott Basin is dominated by high angle faults that have a predominant northeast strike (MacKevett, 1972). To a lesser extent, the basin contains low angle thrust faults and folds. Remarkably, these thrust faults and folds are located above 1,371 m a.m.s.l. throughout the basin and are likely associated with compressional stresses that were exerted as the Yakutat terrane subducted beneath the continental North American plate.

CHAPTER 2 - BACKGROUND

General overview on ice-dammed outburst floods

The earliest records of outburst floods come from Iceland and the Swiss Alps, presumably some of the first glaciated regions to be inhabited. The scientific record and the early emphasis of research in these areas consisted of descriptive narratives largely pertaining to the magnitude and the destructive power of outburst floods (Haeberli, 1983; Thorarinsson, 1939). These early qualitative assessments progressed into more quantitative evaluations when the early investigators began to analyze the physical characteristics of outburst floods. These characteristics included the flooding frequency and the geomorphic and climatic conditions leading up to flooding (Haeberli, 1983).

Starting in the 1950's the emphasis on research became more sophisticated with Thorarison's (1953) research on Grimsvötn and Glen's (1953) work on the stability of ice-dammed lakes and water-filled holes in glaciers. By the 1970's, the physics of subglacial hydraulic features were being outlined (Shreve, 1972; Röthlisberger, 1972; Weertman, 1972). Some of this work was applied to the floods in Iceland. Of note is the research on the outbursts of Grimsvötn by Björnsson (1974) and Nye (1976), the latter of which developed some of the first mathematical models describing outburst flooding. Based on Nye's 1976 work, Clarke (1982, 1996) and Fowler (1999) have made significant advances in mathematically modeling outburst floods.

Glacial hydrology

Glaciologists have recognized two primary types of sub-glacial hydraulic systems, which have been categorized by Raymond et al. (1995) as “fast” and “slow” drainage systems. “Fast” drainage systems are generally comprised of a network of subglacial conduits that have relatively low surface-to-volume ratios and cover very small fractions of the glacier bed (Fountain and Walder, 1998). Fast hydraulic systems may consist of canals incised into basal sediments (Walder and Fowler, 1994), channels incised into bedrock and basal sediments (Nye, 1973); and conduits incised upward into the ice at the glacier bed (Röthlisberger, 1972). “Slow” drainage systems, on the other hand, generally have a relatively large surface-to-volume ratio, and cover a relatively large fraction of the glacier bed (Fountain and Walder, 1998). Slow hydraulic systems can be sub-divided into four distinct types: 1) water films located between ice and bedrock (Weertman, 1972); 2) flow in permeable sediment layers (Stone and Clarke, 1993; Hubbard et al., 1995); 3) braided canals (Walder and Fowler, 1994); and 4) bedrock controlled linked-cavities (Kamb, 1987).

Of the three types of “fast” hydraulic systems, conduits are the most discussed of in the literature. Röthlisberger (1972) assumed conduits as being semi-circular in cross section and incised into the ice at the base of the glacier (Figure 2). The stability of these conduits is a balance between the overburden pressure of the ice collapsing the conduit through creep closure and the counteracting processes of internal water pressure maintaining the opening and wall melting caused by the dissipation of frictional heat of moving water (Röthlisberger, 1972). Moreover, for water above the freezing

temperature, such as in a glacier dammed lake, the heat content of the water also contributes to ice melting (Clarke, 1982). Hence, this interaction between the frictional and thermal melting of the ice walls allows conduits to exhibit an inverse relation between discharge and water pressure (Röthlisberger, 1972). High water discharge results in a high melt-widening rate and the conduit enlarges at a rate that is greater than the rate of creep closure. In this situation the water pressure is low compared to the ice overburden pressure. Conversely, with low water discharge, there is little melt-widening occurring and creep closure dominates, resulting in conduits with small cross-sectional areas and internal water pressures higher than the ice overburden pressure (Shreve, 1972). This condition differs from pipe flow where high water pressures correspond to high discharges and low pressures with low discharges. This inverse relationship for ice-walled channels arises due to increased heat generation associated with increased discharge. Because water tends to flow from areas of high pressure to low pressure, channel development within glaciers assumes an arborescent network, where channels of high pressure drain to channels of low pressure (Röthlisberger, 1972; Shreve, 1972).

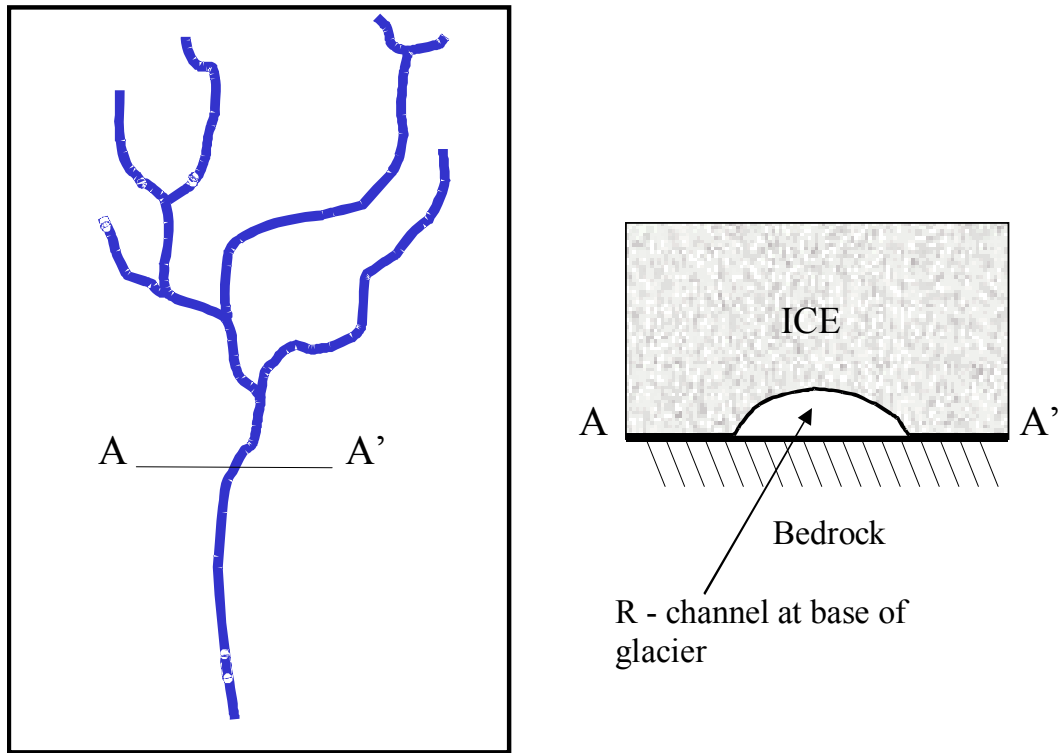


Figure 2. Diagram showing the profile and cross-sectional view of R-channels beneath glaciers.

Röthlisberger (1972) and Shreve (1972) describe the steady-state condition of channels, however, the hydrologic systems within glaciers are seldom in steady-state and change seasonally as well as diurnally (Collins, 1979; Fountain, 1994; Hubbard et al., 1995; Stone et al., 1997). Consequently, water discharge and pressure in channels fed from the surface will tend to be in non-steady state. High water pressures will occur during periods of rapidly rising discharge, when water backs up the system faster than channels can enlarge by melting (Seaberg et al., 1988). Conversely, low water pressures will prevail during rapidly falling discharge, when water leaves the system faster than channels can contract by creep closure. During transient periods of rapidly fluctuating discharge, therefore, high discharges will be associated with high water pressures,

opposite of the inverse relationship for the steady-state condition. Lliboutry (1983) and Hooke (1984) have concluded, however, that because channels enlarge fairly rapidly by melting but close much more slowly by creep closure, the most common condition for non-steady-state systems is one of low water pressure.

The “slow” drainage system involves morphologically distinct flow systems that primarily include subglacial linked-cavities, sediments, and braided canals. Subglacial cavities form as the glacier slides over asperities in the bedrock (e.g. small rock steps and surface irregularities) causing the ice to become separated from the bed (Walder, 1986; Kamb, 1987). Narrow orifices link many of these cavities and form linked-cavity drainage systems (Figure 3). Geomorphic features thought to be remnant cavities have been mapped in previously glaciated areas by Walder and Hallet (1979), Hallet and Anderson (1982), and Sharpe and Shaw (1989). These features consist of small concavities that are preserved in the bedrock. They cover 20-50% of the deglaciated bedrock and are in a non-arborescent configuration.

The mechanics of linked-cavity systems result in very different relationships between discharge and pressure relative to channels, with important consequences for drainage network evolution. Cavity size is a function of the sliding speed of the glacier, the roughness of the glacier bed, and the pressure difference between the ice and water in the cavity (Walder, 1986; Kamb, 1987). Unlike the development of conduits, cavities rely less on the frictional melting of ice due to flowing water. Because of the sinuous nature of the flow paths between cavities, water velocities are small and frictional melting of ice walls is insignificant (Walder, 1986; Kamb, 1987). As a result, increases

in water pressure within the linked-cavity system results in an increased discharge. This positive relationship between discharge and pressure, opposite to that of the conduits, does not drive cavities to coalesce and develop into an arborescent system. As a result, linked-cavity systems tend to be stable features that may store large quantities of water at the base of glaciers but are less likely to play a significant role in rapidly transporting large quantities of water (Humphrey, 1987).

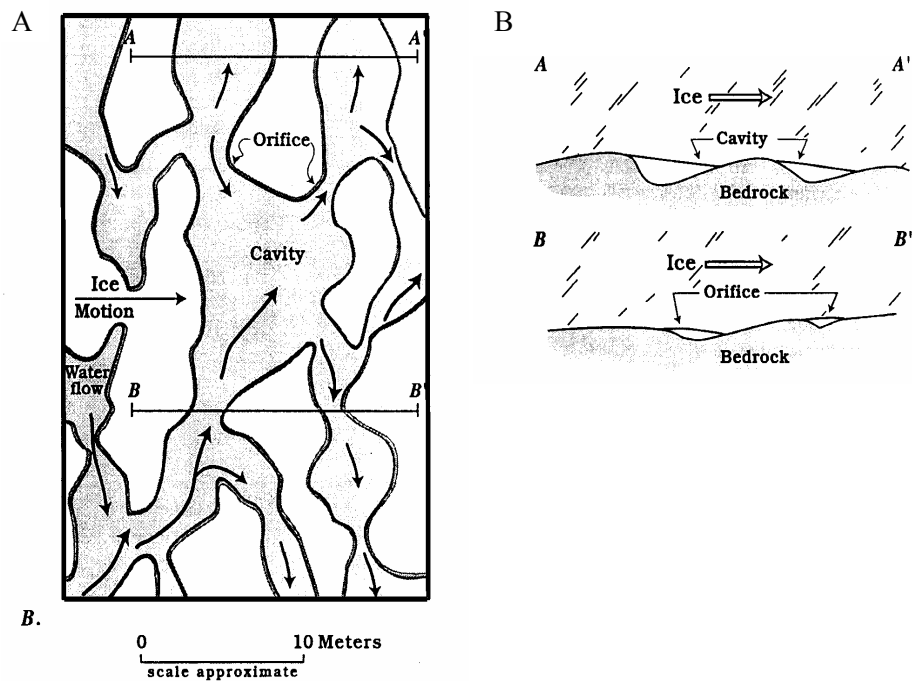


Figure 3. Schematic showing the profile (A) and cross-sectional view (B) of a linked-cavity system (Adapted from Kamb, 1987).

The stability of the linked-cavity system can break down under high pressure and discharge conditions, when frictional heat and ice-melting becomes important factors

(Kamb, 1987). Under such conditions, the linked-cavity system transforms into a system of conduits. This instability provides a mechanism to rapidly evacuate a cavity system of large water volume. This evolution from a “slow” linked-cavity system to a “fast” system of R-channels is thought to play a role in the rapid termination of surging glaciers (Kamb et al., 1985; Raymond et al., 1995).

Another “slow” system is an unconsolidated layer of subglacial sediment that acts as a confined aquifer (Stone and Clarke, 1993). Through in situ borehole tests, Fountain (1994), Hubbard et al. (1995), Stone et al. (1997), and Fischer et al. (1998) have determined that the hydraulic conductivity of these sediments range on the order of 10^{-7} to 10^{-4} m s^{-1} . But in some cases, the hydraulic conductivity may be as high as 0.07 to 0.9 m s^{-1} , comparable to a coarse gravel (Stone and Clarke, 1993). Despite the large range of hydraulic conductivity, subglacial sediment layers do not provide an effective mode of rapidly transmitting large quantities of water due to their thin and laterally discontinuous nature (Nolan and Echelmeyer, 1999a; Nolan and Echelmeyer, 1999b).

Coexisting with the sediment may be sediment-floored canals, whereby water flow can erode the underlying sediment layer by removing particles as both bed load and suspended load (Walder and Fowler, 1994; Fountain and Walder, 1998). Such sediment-floored canals can develop beneath arborescent conduits, or exist at the base of glaciers in a braided, non-arborescent network of wide, shallow, ice-roofed canals.

Release Mechanism

Despite the general acceptance of the “fast” and “slow” subglacial hydraulic systems, how these systems develop, their spatial occurrence, and how they interact is

unclear (Fountain and Walder, 1998). Moreover, how large volumes of water can be stored in glacially-dammed lakes then rapidly drain, such as HCL, is unclear. Scientists typically agree that ice-dammed lake water drains through the glacier via existing tunnels in the ice, enlarging conduits through melt-widening as the flood propagates down glacier (Röthlisberger 1972; Nye, 1976; Clarke, 1982). The crux in this scenario, however, is determining how the seal between the lake and the internal drainage system is ruptured and how a hydraulic connection is made with the glacial hydraulic system. There are currently three principal theories.

The first theory involves the floatation of the ice dam, as discussed by Thorarinsson (1939), Sturm and Benson (1985), Kasper and Johnson (1992), and Knight and Russell (1993). The ice dam floats upward due to buoyant forces imposed by the lake water on the glacier ice. Under normal conditions, clean ice floats when the water depth exceeds 90% of the ice thickness, or, in our case, 90% of the ice-dam thickness. Once the ice dam rises sufficiently it loses contact with the bed, rupturing the impermeable seal, and allows the lake water to connect with an established drainage system. If this theory were true, then outbursts will occur when the lake level reaches 90% of the ice dam thickness. However, most outbursts occur when lake levels are substantially lower (Russell, 1999). In his study of Grimsvötn, Nye (1976) applied a modified flotation explanation and suggested that the ice located on the perimeter of the glacier cantilevered upward through plastic deformation imposed by buoyant forces as the water within the lake raised. This buoyant force reduced the pressure at the base of the ice cap, resulting from the overburden of ice, and caused the hydraulic drainage

divide to migrate towards the lake. When the divide reached the lake, water leaks out initiating a flow that would unstably enlarge a conduit resulting in a flood.

An alternative triggering mechanism has been presented by A. Fountain and J. Walder (personal communication, 2000). They postulate that a network of subglacial conduits is enlarging coincident with the increasing melt as the summer progresses. At some point the conduit network reaches the lake, and a runaway flood proceeds by melt-widening of the channel system. Thus, the timing of the outburst is related to lake level and to the location and enlargement of the “fast” conduit network. In this regard, the up-glacier development of the “fast” conduit system appears to correlate with the seasonal, up-glacier migration of snowline (Nienow, 1994).

The third drainage mechanism evolves the destabilization of subglacial cavities. Knight and Tweed (1991) hypothesized that glacier movement may separate the glacier from its bed and thereby enhance rapid cavity development at the ice/bed interface, and in the presence of high water pressure (such as a glacially impounded lake), the cavity system destabilizes and a connection between the lake and the “fast” hydraulic system is made.

Past work related to the Study Area

Only two formal studies of the outburst floods of HCL are known. Friend (1988) studied HCL for one field season in 1986. He made measurements of the volume and temperature of HCL, and measured outflow hydrographs as the floodwaters flowed past the town of McCarthy. Friend attempted to correlate his measured hydrographs to

results derived from two mathematical models, the first developed by Clague and Mathews (1973) and the second by Clarke (1982). The Clague and Mathews model is an empirical model used to estimate peak discharge based on the peak lake volume, and the Clarke model is a physically-based numerical algorithm that predicts the flood hydrograph. The results of Friend's (1986) work showed large discrepancies between his measured peak discharge values with estimates obtained by the two models. He attributed this discrepancy to natural variability unaccounted for by the two models and to his own measurement errors.

Rickman and Rosenkrans (1997) examined the flood history of the lake. As part of their effort they gathered and reviewed aerial photos and historical records dating back several decades, surveyed the lake bathymetry, estimated past lake stages, and constructed outflow hydrographs of Kennicott River at the glacier terminus for the 1994 and 1995 outburst floods. As a result of their research, they compiled a flood history for HCL dating as far back as 1900. This flood history consists of a list of outbreak times developed through direct observation and anecdotal evidence from residences of the town of McCarthy and people affiliated with Kennecott mine. From this historic record, they concluded that the maximum annual lake stage is declining with time and attribute this decline to glacial thinning. Lastly, Rickman and Rosenkrans developed a list of indicators forewarning of an imminent flood:

- Lake stage near or above 914.4 m a.s.l.
- Stationary or declining lake stage during the period in which melt water and rain would be expected to be increasing lake stage (July and August).
- Evidence of recent calving of large ice blocks from the glacier.

- Formation of a “clean ice” washline along the ice margin. This is visible after a small drop in lake stage.
- Fresh fractures and escarpments in the ice margin region.

CHAPTER 3 – SNOW ACCUMULATION AND RUNOFF MODEL

Introduction

In this chapter I address hypothesis 1 by testing whether the timing of outburst correlates with the meteorological variables, temperature and precipitation, and other variables including changes in lake level and the development of a “fast” hydraulic system. To evaluate temperature and precipitation, I assume both are indexes to runoff entering HCL and apply two simple mathematical analyses to test their correlation against outburst timing. To determine the effects of changing lake level and the development of a “fast” hydraulic system, I use information obtained from a hydrologic model that was specifically developed for the HCL basin and the Kennicott Glacier. The development of this model is outlined in this chapter. In particular, the model is used to estimate lake level by predicting cumulative daily runoff entering HCL. In addition, following Nienow’s (1994) work, the model is used to approximate the location of the “fast” hydraulic network by estimating the time at which the snowline exceeds the elevation of HCL and correlating it to the time of outburst.

The correlation analyses discussed in this chapter were performed on fourteen of the most accurately dated floods from the historic record (Rickman and Rosenkrans, 1997). Only those floods directly observed were used; the floods whose timing was based on anecdotal evidence were discarded.

Correlating outbreak timing to meteorological variables

To evaluate if the volume of water stored behind the dam (and with it lake stage) has a controlling effect on outbreak timing, I treated temperature and precipitation as indexes of runoff entering the lake and performed correlation analyses between them and the release date of fourteen of the most accurately dated floods. In this approach, I assume temperature and precipitation are indexes of runoff due to their influences on melt runoff and runoff due to rain, respectively.

Baseline meteorological data for this study, including temperature and precipitation, were obtained from the closest meteorological station to HCL, known as McCarthy 3SW (National Climate Data Center's Identification Number 505757). McCarthy 3SW is about 381 m a.s.l. and is located about 1.5 km southwest of the terminus of Kennicott Glacier at a latitude of 61°35' N and a longitude of 143°00' W. The meteorological variables recorded at the station include daily precipitation, snowfall, snow depth, maximum and minimum air temperature, and the temperature at the time of observation. Data for the water years from 1968 to present are available through the National Climate Data Center's web page (<http://www4.ncdc.noaa.gov>).

To evaluate the role of temperature, a degree-day index was used. This index consists of the cumulative summation of mean daily temperatures (average of daily maximum and minimum values) above freezing. In this analysis, the degree-day index was computed from September 1 to July 1. The September 1 date was elected because, according to Rickman and Rosenkrans (1997), the lake is generally empty or just starting to refill after outbreak at this time. I assume that the lake is empty on

September 1, and the ice dam forms a perfect seal. The July 1 date was used as the end date since this date precedes the earliest release date of July 4 in 1993. The July 1 date has no other particular significance. The data were not summed to the release date because the degree-day sum would be self correlated with the outbreak date. That is, the longer the outbreak delay, the greater the magnitude of the degree-day sum.

To evaluate the effects of precipitation and determine the effect of runoff due to rain alone, a cumulative sum of precipitation was calculated from September 1 to July 1 for each flood season.

Values from both the degree-day index and the sum of cumulative precipitation were plotted against the time of outbreak (Figures 4 and 5, respectively). Based on the high degree of spread present in both plots, it can be concluded that there is no correlation between temperature and precipitation to the time of outbreak. This conclusion can be substantiated by the low valued regression coefficients for each plot and the inability of the correlation coefficients to be significant at the 90% confidence level (Table 1 and 2).

Table 1. Correlation of date of outbreak with cumulative degree-day index. July 1 is Julian Day 182.

Year	Date of Outbreak (Julian Day)	Degree-day sum From Sept 1 to July 1	Correlation Coefficient	t-statistic	t-critical at 90% significance level
1974	228	3852	0.02	0.08	1.36
1975	218	3878			
1978	221	4072			
1981	200	4106			
1986	217	3245			
1988	199	4116			
1989	200	3702			
1993	186	3531			
1994	209	4196			
1995	201	4226			
1997	221	3769			
1998	222	3918			
1999	196	3672			

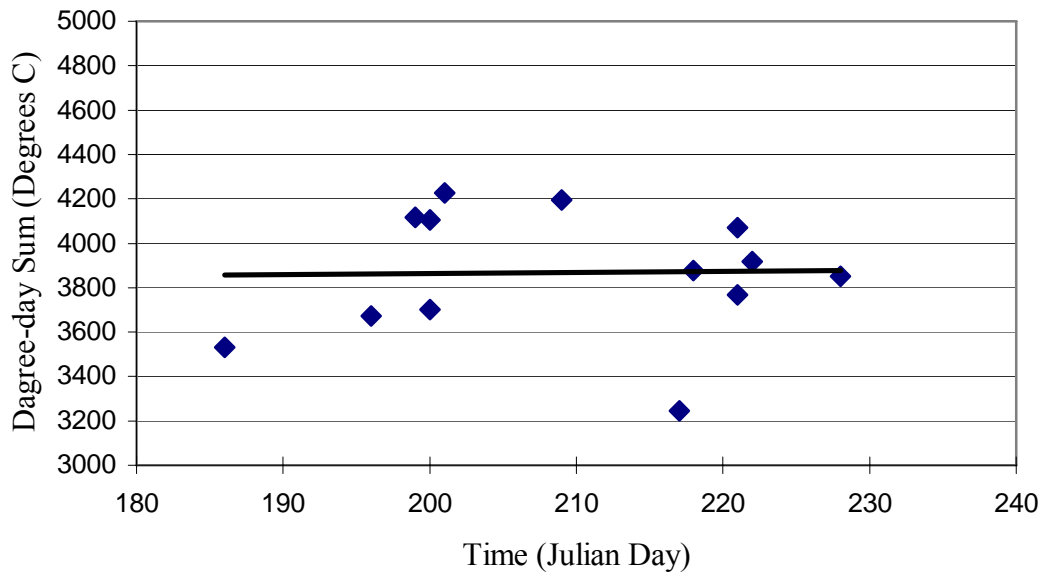


Figure 4. Plot of degree-day sum against the day of outbreak.

Table 2. Correlation of date of outbreak with the total precipitation falling at Hidden Creek Lake from September 1 to July 1.

Year	Date of Outbreak (JD)	Total Precipitation (cm) from September 1 to July 1	Correlation Coefficient	t-statistic	t-critical at 90% significance level
1974	228	69	-0.15	-0.52	1.36
1975	218	119			
1978	221	94			
1981	200	127			
1986	217	112			
1988	199	117			
1989	200	102			
1993	186	74			
1994	209	107			
1995	201	81			
1997	221	64			
1998	222	69			
1999	196	71			

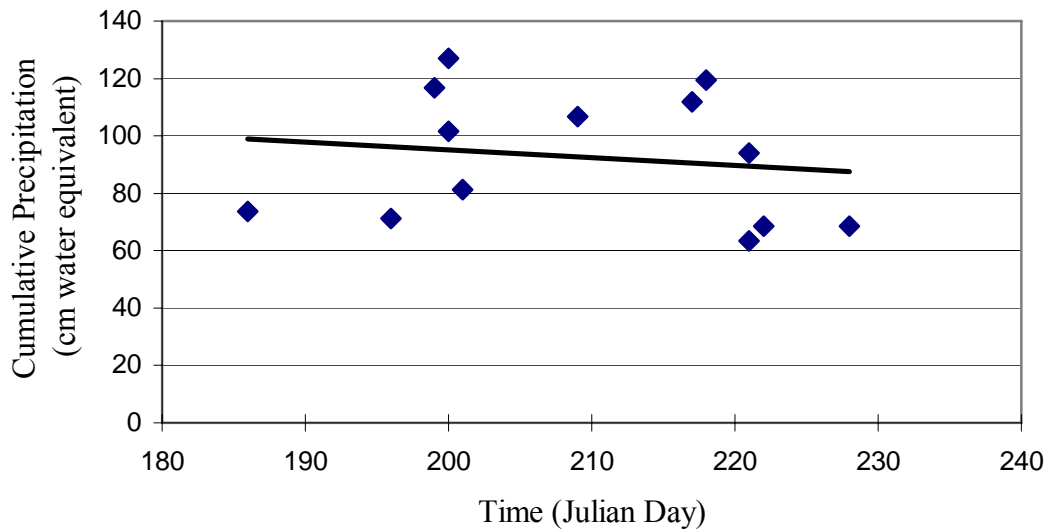


Figure 5. Plot of cumulative precipitation to date of outbreak.

Hydrologic Model

To evaluate the correlation of lake level to the time of outbreak, and test whether there is a correlation between the location of the “fast” hydraulic system and the time of outbreak, a hydrologic model was developed. This model is a simple model that utilizes temperature and precipitation as input data to calculate snow accumulation, ablation within the HCL basin, and to calculate runoff entering the lake. Other, more robust models using elaborate algorithms and more complex input data are available (Melloh, 1999). However, our situation of limited meteorological data dictates that a relatively simple model is used.

In the following section I introduce the model and discuss the mechanics of how it estimates snow level and runoff within the HCL basin. This is followed by a test of the model’s ability to estimate runoff within a gaged basin, known as the Little Susitna Basin, prior to its application to HCL. Note that the units in the model are English because the equations in the model were developed with English units and require their use. The final values obtained by the model are converted into metric units.

Model Overview

The mechanics of the model start by separating the basin into different elevation zones. For each elevation zone the model predicts the depth of snow accumulation and melt using only the measured variables, precipitation and temperature, which themselves are dependent on elevation. By summing the total snowmelt and rainfall occurring at each elevation zone, the total volume of runoff from within the basin is estimated. No routing of water is calculated, and all available water is assumed to enter the lake basin instantly. Because of this assumption of instantaneous routing, I am not

accounting for the natural short-term attenuation of flows that occur along the path from the point of origin to the lake. Consequently, I expect the daily values of runoff to exhibit sizable errors. However, because I am only interested in evaluating the cumulative runoff entering the lake over an entire season, the high day-to-day variability will be buffered and the error over the season should have a lower degree of error. A detailed flow chart of the model is provided in Figure 6.

Calculating Precipitation at Elevation

The Kennicott River basin is located in a rain shadow caused by the Chugach Mountains to the south, which buffers the basin from weather fronts originating in the Gulf of Alaska (Personal Communication, Dr. C. Daly of Oregon State University, Corvallis, winter 2000). Aside from the McCarthy 3SW station, there are no other weather stations located within the Kennicott Glacier basin. Thus, to assess and correct for differences in precipitation occurring up the Kennicott Glacier basin, as a result of the local anomalies in the weather patterns and the natural increase in precipitation with elevation, information from a publicly available Parameter-elevation Regression on Independent Slopes Model (PRISM) was used. Developed by Dr. Daly (www.ocs.orst.edu), the PRISM model uses point climatic data, a digital elevation model, and other spatial data sets to generate gridded estimates of climate parameters such as precipitation, temperature, and snowfall.

From PRISM, average annual precipitation was calculated at different grid points along a transect originating at the McCarthy weather station and extending north up the west side of the Kennicott Glacier and through the HCL basin (Figure 7). This process exhibited a linear relationship of about 14 inches (36 cm) of increased precipitation for

every 1000 feet (305 m) gain in elevation. The precipitation recorded at the McCarthy station was then scaled for the basin using this relation with elevation.

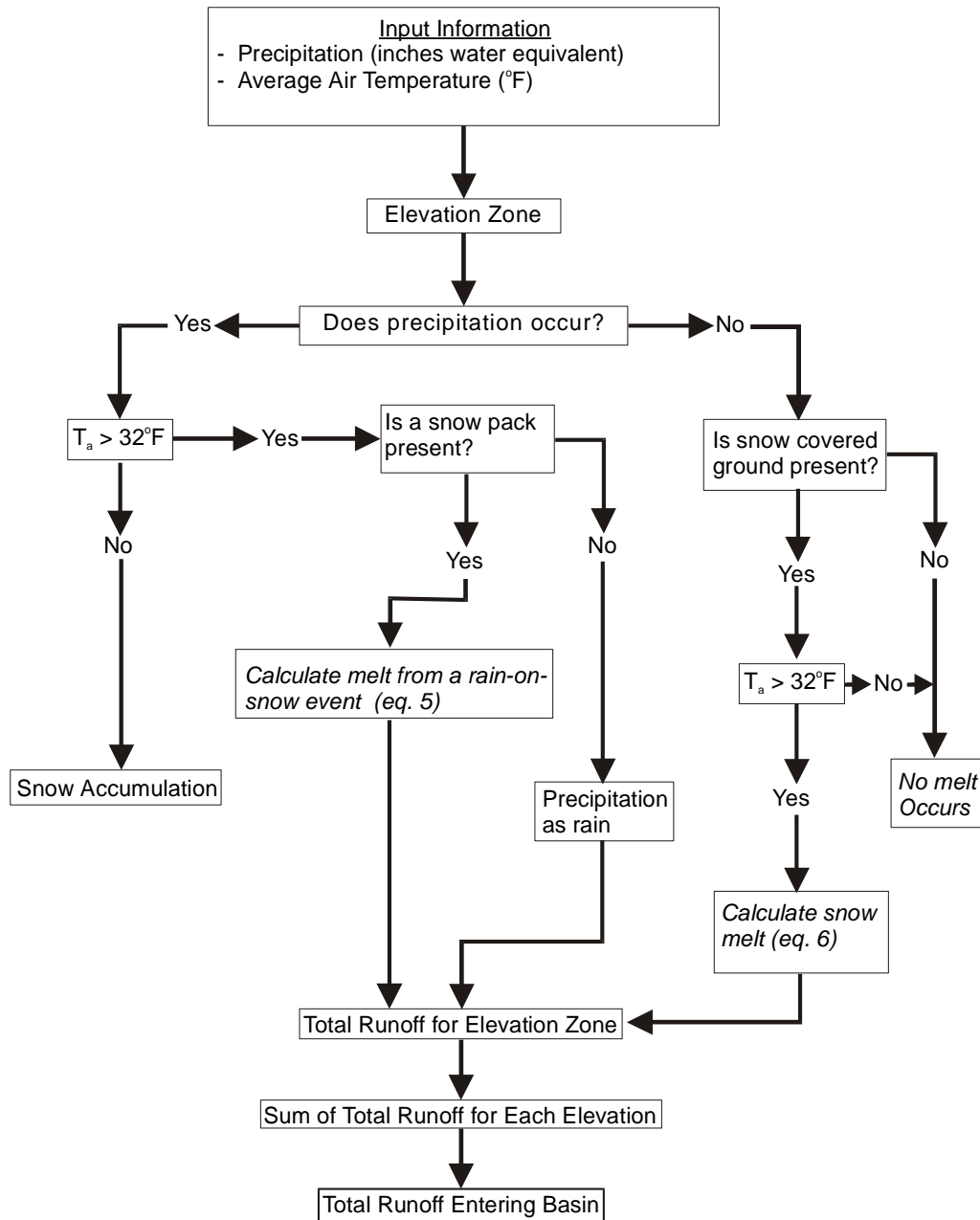


Figure 6. Flow chart of runoff model.

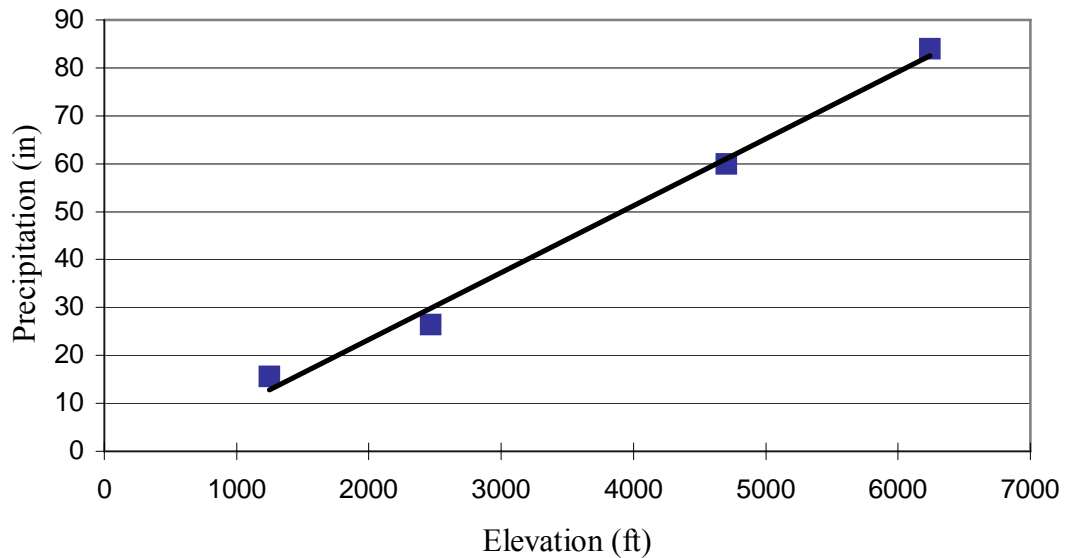


Figure 7. Plot of precipitation with increasing altitude up the Kennicott Glacier valley. Information obtained from PRISM.

Calculating Temperature at Elevation

To determine whether the precipitation reaches the ground as snow or rain, the average daily air temperature (T_a) at each elevation has to be known. It is assumed that when $T_a > 32^\circ\text{F}$ the precipitation is rain, and when $T_a \leq 32^\circ\text{F}$ the precipitation is snow. The average daily air temperature was calculated by averaging the daily-recorded maximum and minimum temperatures from the McCarthy weather station. The average daily air temperature at higher altitudes was estimated using the adiabatic lapse rate of -0.78°F per 328 feet (100 m). This lapse rate is commonly applied by the USGS in this portion of Alaska (Personal Communication, Dennis Trabant, 2-24-00), and is also found in published data (Donn, 1951).

Calculating Snowmelt

To estimate snowmelt, some estimate of energy transfer is required. The energy balance equation for melting snow (Anderson, 1968, 1973; U.S. Army, 1960; and Melloh, 1999) is,

$$Q_n + Q_e + Q_h + Q_{px} = M, \quad (1)$$

where Q_n is net solar radiation transfer; Q_e is latent heat transfer; Q_h is sensible heat transfer; Q_{px} is heat transfer by rain water; and M is the energy available to melt ice. Anderson (1973) provides a detailed discussion of each component of the energy equation. Given the data available for our situation, the model relies on two simplified equations to evaluate snow melt during rain-on-snow and rain-free conditions.

Heat transfer during a rain-on-snow event involves the following basic considerations (U.S. Army, 1960). Net solar radiation is composed of two terms, net short-wave (Q_s) and net long-wave (Q_l), and the melt produced by each can be expressed differently. Melt due to net short-wave radiation is relatively unimportant during periods of rain and is considered to amount to about 0.07 inches of snowmelt per day for non-forested areas such as in the HCL basin. Melt due to the exchange of net long-wave radiation (M_{rl}) between forests or low clouds and the snowpack may be computed as a linear function of air temperature,

$$M_{rl} = 0.029(T_a - 32) \quad (2)$$

where T_a is mean air temperature in °F.

Melt generated by the transfer of sensible heat as warm air is advected over the snow surface (convection), and melt generated by the transfer of latent heat as water

vapor from the atmosphere condenses on the snow surface (condensation) can be combined into one term of snow melt (M_{cc}). Assuming that air is saturated during rain on snow events (i.e. the mean air temperature is equal to the dew point), M_{cc} is expressed as,

$$M_{cc} = (k)0.0084V (T_a-32) \quad (3)$$

where V is the average wind velocity in miles per hour at a height of 50 feet off the snow surface and k is a basin constant that represents the mean exposure of wind. The value of k can range from 0.3 to 1 for heavily forested areas and unforested areas, respectively.

Melt due to the transfer of heat from rain (M_p) is simply expressed as a function of rainfall and air temperature,

$$M_p = 0.007P_r (T_a-32) \quad (4)$$

where P_r is daily rainfall in inches.

Lastly, melt due to heat exchange at the snow-soil interface is negligible compared to the heat exchange at the snow-air interface (Anderson, 1968, 1973; Melloh, 1999). Therefore, calculations of melt due to geothermal heat were not made, but were assumed constant at 0.02 inches per day (U.S. Army, 1960).

After assuming that water lost by sublimation is balanced by condensation, and the effects of heat exchange within the snowpack during non-melt periods are negligible, equations (1) through (4) can be combined into a general equation representing the total melt for rain-on-snow events (U.S. Army, 1960),

$$M = (0.029 + 0.0084kV + 0.007P_r)(T_a - T_b) + 0.09 \quad (5)$$

where M is total daily snowmelt in inches per day, and T_b is the base temperature at which melt will occur. Expressions similar to Equation (5) appear in the work of Anderson (1973) and Harr (1980).

For my application, k and T_b are set at 1°F and 32°F, respectively. The airspeed, V , is set at approximately 4.5 mph based on average winter wind speed observations made approximately 50 feet from the surface of the Gulkana Glacier, which has similar geographic and topographic conditions as those found at HCL (personal communication, Dennis Trabant, USGS).

On clear days, net solar and terrestrial radiation become more important variables in the energy balance equation than on cloudy, rainy days, and additional input variables are required to calculate snowmelt. These additional variables include average basin forest canopy coverage, solar radiation, albedo, snow surface temperatures, and dew point (U.S. Army, 1960; Melloh, 1999; Anderson, 1973). Because air temperature and precipitation are the only variables available for our model, a more simplified method of calculating snowmelt for clear periods was applied. This method is referred to as the degree-day index method, and is represented by the following equation (Melloh, 1999),

$$M = C_d (T_a - T_b) \quad (6)$$

where M is snowmelt (in./day), C_d is degree-day melt coefficient (in. °F⁻¹ day⁻¹), T_a is average daily air temperature (°F), and T_b is the temperature at which melt will occur (°F). The values of C_d and T_b are set at 0.06 and 24°F, respectively, and equal to values

for open, non-forested areas (U.S. Army, 1960). In forested areas, the vegetative cover affects the transfer of energy produced by net solar radiation and sensible heat by shading the snow pack and disturbing local wind patterns. Consequently, snowmelt can occur at lower temperatures in open areas resulting in the use of T_b equal to 24°F, rather than 32°F used in forested areas.

Equation (6) relies on a fixed melt factor. This differs from Anderson (1973) who used a melt factor that varied seasonally with fluctuations in solar influences and snowpack conditions. The varying melt factor could not be applied in this model because no information on the snowpack's characteristics exist. In addition, snowpack sublimation is not included in the model because to calculate snowpack sublimation with reasonable accuracy is difficult without detailed information of the local dew point and wind velocities (Anderson, 1973). However, since sublimation loss is generally very small, by not accounting for it will not likely have a significant affect on the overall error within the model, which is likely many times larger.

To summarize, the model uses the precipitation and temperature data from the McCarthy weather station as input. Precipitation is scaled for different elevations using the PRISM correction. Temperature is scaled using the lapse rate. Snow accumulation and ablation (snow levels) and water flow at different elevations in the basin are calculated based on direct rainfall and snowmelt, if present, using equations (5) and (6).

Testing the Runoff Model

The runoff model was tested against a gaged basin, the Little Susitna River basin, located in the Talkeetna Mountains north of Palmer, Alaska, approximately 325 kilometers west of HCL (Figure 8). The Little Susitna River ranges in elevation from

279 m a.s.l. to approximately 1981 m a.s.l., has a drainage area of 160 km², and is only slightly covered by forested areas.

The Little Susitna River was chosen as a test candidate over other gaged basins for several reasons: 1) the Little Susitna River has similar meteorological characteristics to Hidden Creek basin, as determined by PRISM data; 2) it has similar physiographic characteristics to HCL; and 3) there is a comprehensive record of discharge and meteorological data available for the Little Susitna River since the early 1950's. Discharge of the Little Susitna River has been gaged by a USGS gage station (USGS Station number 15290000) and meteorological data are collected approximately 12 km (7.5 mi.) away in the town of Palmer (National Climate Data Center Number 506870).

In order to maximize computational efficiency while still accounting for meteorological fluctuations at different elevations, the Little Susitna River basin was subdivided into six elevation zones. Precipitation was scaled for each zone based on information provided by the PRISM model (Table 3), and temperatures were scaled for each elevation zone using the same adiabatic lapse rate as previously discussed. Using these adjusted precipitation and temperature measurements, the model calculated the daily discharge of the Little Susitna basin for 10 water years from 1975 to 1988 (Table 4). Years with missing data over this time period were not included.

Table 3. Little Susitna River area distribution and enhancement factors.

Elevation interval in feet (meters)	Mid altitude in feet (meters)	Area in miles² (km²)	Precipitation Enhancement Factor
Station – 2000 (610)	1500 (457)	4.0 (10.4)	1.79
2000 (610) – 3000 (914)	2500 (762)	12.4 (32.2)	2.49
3000 (914) – 4000 (1219)	3500 (1067)	20.1 (52.2)	3.19
4000 (1219) – 5000 (1524)	4500 (1372)	18.4 (47.7)	3.89
5000 (1524) – 6000 (1829)	5500 (1676)	6.0 (15.5)	4.59
> 6000 (1829)	6200 (1890)	0.2 (0.4)	5.08

Table 4. Total discharge calculated using runoff model compared to the gaged volume of Little Susitna River.

Year	Gaged Volume (km³)	MET Model Volume (km³)	Difference (km³)
1988	0.150	0.149	0.001
1987	0.189	0.159	0.030
1986	0.146	0.146	0.000
1985	0.270	0.126	0.144
1984	0.219	0.142	0.077
1982	0.235	0.159	0.076
1980	0.263	0.227	0.037
1979	0.230	0.137	0.093
1978	0.127	0.119	0.008
1977	0.223	0.248	-0.025
Average	0.203	0.208	Root Mean Square= 0.032 km ³

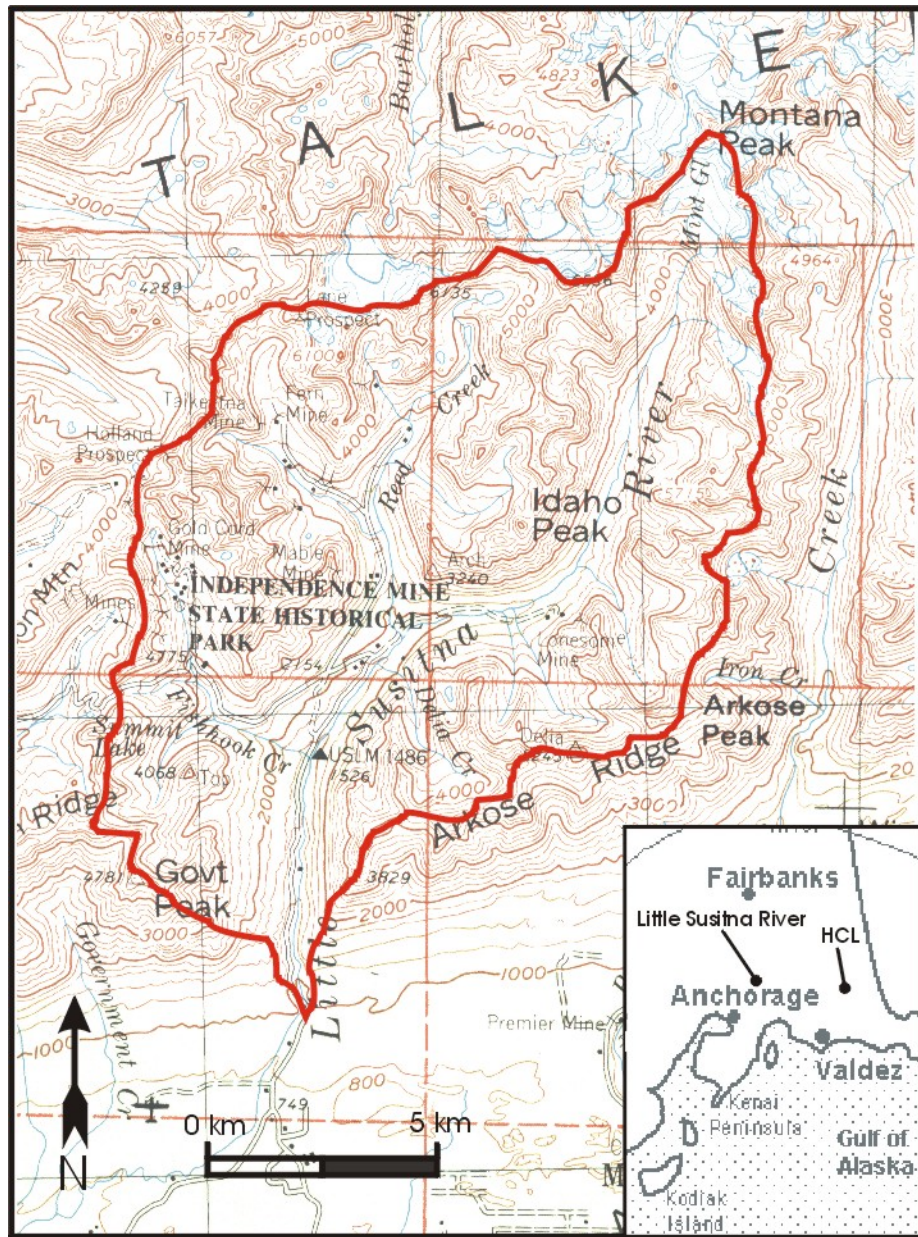


Figure 8. Illustration showing the location of the Little Susitna River basin.

The results within Table 4 were plotted (Figure 9). Looking at the plot you can see that there is significant variability in runoff that is not accounted for by the simple model. This is confirmed by the inability of the correlation coefficient to be significant at the 90% confidence level, with a t-statistic of 1.31 falling just inside the t-critical value of 1.39. The year-to-year variability yields a root-mean-square of 0.032 km^3 , and the standard deviation of percent error values equates to a model accuracy of $\pm 21\%$. For such a simple hydrologic model, this error magnitude is not uncommon (Rana et al., 1996; Marks et. al., 1999).

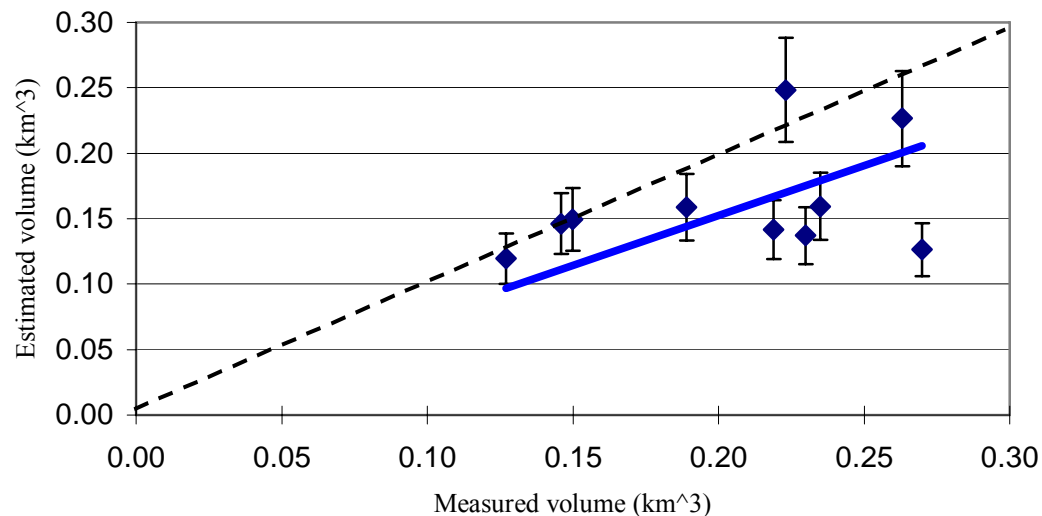


Figure 9. Plot of modeled discharge volumes compared to measured discharge volumes for 10 water years on the Little Susitna River. The line fit to the results is through the origin and the error bars indicate $\pm 21\%$ error.

To assess the influence of each individual input variable, a sensitivity analysis was performed on the model. This involved increasing the three primary input variables, precipitation, temperature, and wind velocity, individually by 2% and determining how

cumulative runoff is affected. This test was performed on the Little Susitna River basin for water year 1977. Of all three input variables, precipitation proved to be the most influential by returning the largest increase in cumulative runoff with an increase of 2.9% over initial values (Table 5). This increase in runoff is the result of a direct increase in runoff as rain when temperatures are above freezing (Spring through Fall months) followed by a dramatic increase in snow accumulation during the winter. This increased snow pack almost completely melts off when subjected to rain-on-snow events in the spring. The effects of increasing precipitation exceeded those obtained by raising temperature, which resulted in a 2% increase in cumulative runoff. This reduced effect is due primarily to the inability of temperature to directly increase the volume of precipitation falling. Raising temperature only allows less snow to accumulate in the fall and more snow to melt in the spring when temperatures are hovering around freezing. At any other point in the season, the temperatures are either too cold or too warm to allow a slight 2% increase in temperature to dramatically alter the accumulation or melt of snow. Lastly, wind speed, which influences melt by affecting heat exchange properties at the surface of the snow pack, was the least influential with an increase in runoff of less than 1%.

Table 5. Results of a sensitivity analysis performed on the input variables of the runoff model.

Temperature	Precipitation	Wind Velocity	% change in runoff over initial volume
2% Increase	No Change	No Change	2.0%
No Change	2% Increase	No Change	2.9%
No Change	No Change	2% Increase	0.04%

By applying the model to the gaged basin of Little Susitna River, we were able to assess the accuracy of the model, as well as determine the influences that individual input variables have on the model. Consequently, it has been determined that, although there failed to be a significant linear trend between the modeled and measured runoff volumes, the standard deviation in error between the two values is at a reasonable $\pm 21\%$. Based on the sensitivity assessment, some of this error may be attributed to inaccuracies in the quantity and spatial distribution of precipitation within the basin. Knowing the accuracy of the model and its sensitivity to precipitation, the model was applied to the HCL.

Application to Hidden Creek Lake

The Hidden Creek basin was divided into roughly equally spaced elevation zones, each encompassing approximately 1000 feet (305 meter) of vertical elevation, and precipitation enhancement factors from McCarthy station were calculated using information obtained from PRISM (Table 6). Stratifying the basin into 1000-foot (305 meter) elevation intervals allows us to more accurately calculate the effects of snow accumulation and melt with elevation, without overwhelming the computational effort. The area of each elevation zone presented in Table 6 were calculated using GIS (ArcView 3.2) software. It is assumed that the lake is empty on September 1 of each year and a perfect seal exists. Daily runoff entering the lake is calculated from September 1 to the day of outbreak. Thus, lake volume at the time of outbreak is the cumulative sum of all runoff occurring since September 1 of each year.

Table 6. Hidden Creek basin area distribution and enhancement factors.

Elevation interval in feet (meters)	Mid elevation in feet (meters)	Area in miles² (km²)	Precipitation Enhancement Factor
Lake – 3500 (1067)	3250 (991)	2.2 (5.8)	2.6
3500 (1067) – 4500 (1372)	4000 (1219)	3.9 (10.0)	3.3
4500 (1372) – 5500 (1676)	5000 (1524)	8.1 (21.0)	4.2
5500 (1676) – 6500 (1981)	6000 (1829)	10.4 (27.0)	5.1
> 6500 (1981)	7000 (2134)	2.1 (5.6)	6.0

To determine the model's accuracy in estimating the volume of HCL, the calculated cumulative volume of runoff at the time of outbreak was compared to estimated lake volumes. The estimated lake volumes were obtained by interpolating along a volume versus elevation curve (storage curve) that was developed from the lake hypsometry (area versus elevation distribution). The lake hypsometry was determined with the help of Mr. Trabant and Ms. Cunico (Figure 10). A storage curve (dV/dh) was obtained by interpolating along the hypsometric curve (dA/dh) at evenly spaced intervals of elevation, cumulatively adding the volumes, and expressing the result over elevation (Figure 11). With the volume versus elevation curve, lake stage information could easily be converted to lake volume. The only years where the lake stage was surveyed just prior to outburst for HCL included the three flood seasons of 1994 and 1995, with the work completed by Rickman and Rosenkrans (1997), and 1999, with the work completed as part of this thesis. The results of the model are poor (Table 7).

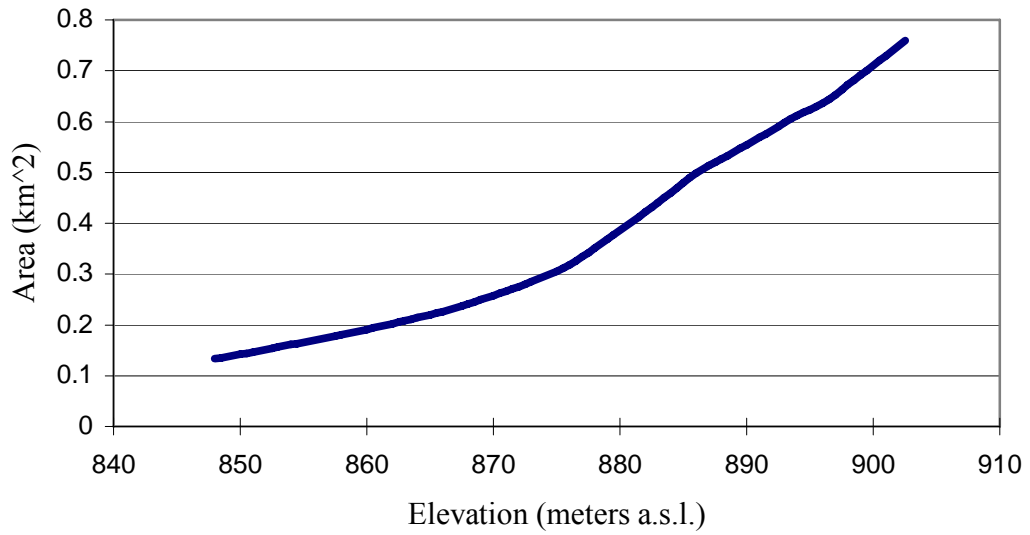


Figure 10. Area versus elevation (hypsometry) distribution of Hidden Creek Lake.

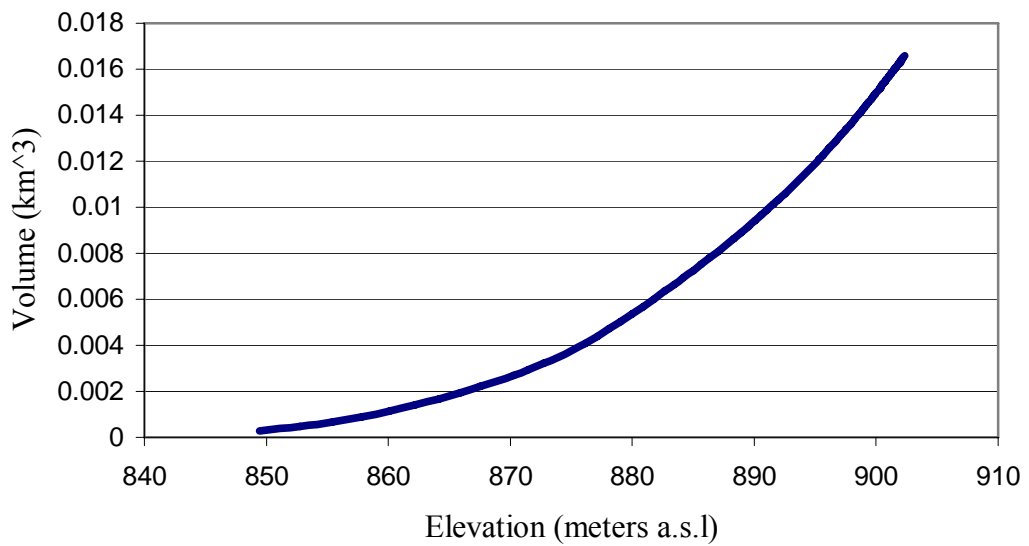


Figure 11. Volume versus elevation distribution of Hidden Creek Lake.

Table 7. Measured and calculated lake volume compared

Year	Volume (10 ⁶ m ³)	Model Volume (10 ⁶ m ³)	Difference (10 ⁶ m ³)	% Difference
1999	0.017	0.073	-0.057	-341
1995	0.033	0.098	-0.065	-197
1994	0.040	0.115	-0.075	-187

A linear regression between the modeled and estimated volumes yields a slope of 1.7 and a y-intercept of 0.043 km³ with a regression coefficient of 0.99 (Figure 12).

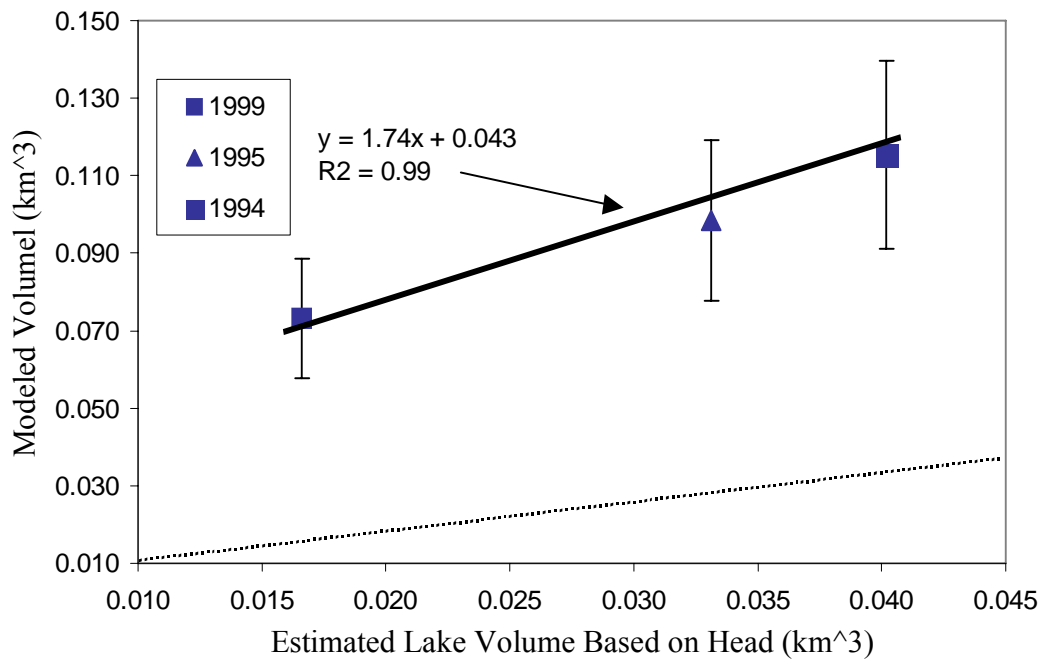


Figure 12. Comparison of estimated lake volumes against modeled lake volumes.

Although the regression line provides a significant fit, it does not have an optimum slope of one, which would occur in the case of a perfect match between estimated and modeled volumes. Moreover, it is apparent that the model is over estimating the lake volume. Factors contributing to this overestimation are errors in the model, errors developed in extrapolating precipitation levels to the Hidden Creek basin from McCarthy, and in developing the hypsometric curve. An additional drawback, which may provide a false perception of model error, is the inability to compare the model to more than just three years of lake level data. Ideally, the more years to compare to the better a determination of the model error can be made.

To apply the model to HCL, I corrected the model output by subtracting the intercept of the regression equation to shift the equation so that it passes through the origin. Such a dramatic correction is not unusual to generalized hydrologic models. In fact, the U.S. Army Corps of Engineers' HEC-1 and HEC-2 surface water models utilize a dimensionless coefficient to account for variation from the generalized snowmelt equations, which are the same equations used in this model (Melloh, 1999). The results of this correction are presented Figure 13. After correcting the model, the error bars depicting the $\pm 21\%$ model error, as determined from modeling the Little Susitna River basin, nearly overlap the line with an optimum slope of one. The remaining analyses are based on this correction.

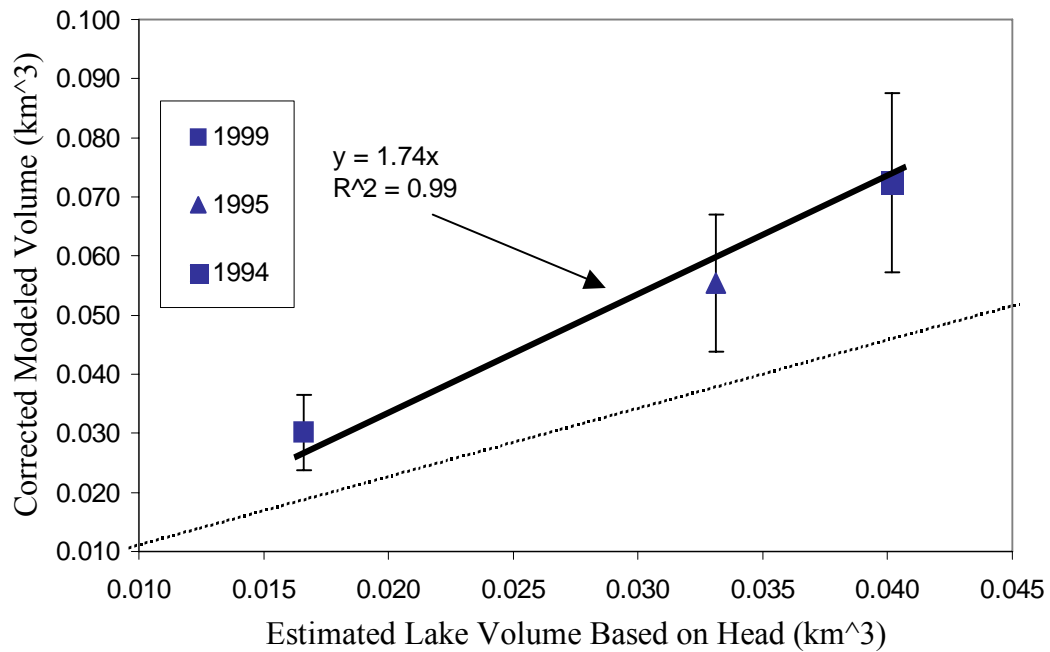


Figure 13. Comparing estimated volumes to corrected modeled volumes.

Analyses

As indicated, the principle goals of developing the hydrologic model were to test Thorarinsson's (1939) flotation and Nye's (1976) cantilever theories, and to determine if the snowline correlates to the time of outbreak by using it as an indicator of the location of the 'fast' hydraulic system in the proximity of HCL. Where appropriate, the modeled results were examined for thirteen of the most accurately dated flood events from the historic record (Rickman and Rosenkrans, 1997).

Testing the Flotation and Cantilever Mechanisms

Thorarinsson's flotation (1939) and Nye's cantilever mechanisms (1939) rely on the water elevation reaching a certain threshold before outbreak can occur. Basically, the

buoyant force applied to the ice dam is proportional to the depth of water located behind the dam. To determine if a critical lake level exists, I examined the maximum lake stage occurring at the time of outbreak: if the ice thickness is constant then a constant critical level exists.

The volume of runoff entering the lake from September 1 to the time of outbreak was estimated using the hydrologic model. Lake levels were then obtained by interpolating along the volume versus elevation curve (Figure 11). The values of peak lake water level obtained by this method are presented in (Table 8). Results indicate that lake level at the time of outbreak does not correspond to one particular elevation, but varies from 913 m in 1999 to 935 m in 1975, with the average head being approximately 926 m. Given the variability of head values over the past 25 years, it would appear that there is no flotation threshold for HCL. However, because of possible errors in the models ability to accurately calculate the volume entering the lake, which are assumed to result in an error of about ± 4 m of lake head, it can not be decisively

Table 8. Estimates of water level for 13 of the most well-known flood events from Hidden Creek Lake. The expected error in water elevation is ± 3.5 m.

Year	Water elevation (m a.s.l.)
1974	921
1975	935
1978	929
1981	934
1986	932
1988	927
1989	925
1993	915
1994	928
1995	923
1997	926
1998	924
1999	913

conclude that this is the case. Regardless of these errors, the lack of a threshold condition existing may be corroborated by the lack of a correlation between the time of outbreak and the key meteorological variables, temperature and precipitation, that control runoff entering the lake.

Examining water level as a function of year (Figure 14), there appears to be a trend towards outbursts at lower lake levels. Over the last 25 years, the inferred peak water level at the time of outbreak has lowered by about 9 meters. This decreasing trend could be the result of a reduction of ice dam thickness.

After considering the density difference between clean glacial ice (900 kg m^{-3}) and water at 0°C (1000 kg m^{-3}), the 9 m decline in head may imply that there has been an approximately 10 m decrease in ice thickness since 1974. It is assumed that density differences in the glacier as a result of crevassing (making it less dense) and debris located within and on the surface of the glacier (making it more dense) offset one another.

To determine if glacial thinning is important, several aerial photos (1975, 1984, and 1999) were examined. Surface elevation can not be determined from the photos, but changes in lateral extent of the glacier can be detected. Presuming that thinning ice will cause the glacier edge to move toward the center of the glacier, I compared locations of the upper surface of the glacier to several established points along the perimeter of the glacier, including rock outcrops near the re-entrant zone of HCL. No distinguishable change in ice extent was observed since 1975. This examination may be inconclusive because the valley walls near the glacier in this area are quite steep, and

small changes in thickness may not be readily observable as changes in lateral extent. I then compared our survey data of the glacier surface to elevations based on 1957 aerial photographs and published on the 1959, USGS McCarthy (C-6), 1:63,360 quadrangle. The average difference in surface height of the glacier at the latitude of HCL is about 42 m. This is equivalent to a thinning rate of 1 m yr^{-1} from 1957 to 1999. This rate of decline is close to a 1.1 m yr^{-1} thinning at the terminus of the glacier, where survey data show a 53 m vertical drop in the ice surface over a 48 year time span from 1909 to 1957 (Rickman and Rosenkrans, 1997). I therefore estimate a 25 m thinning at the ice dam. Again, after taking the density difference between ice and water into consideration, this 25 m decline in ice dam thickness would equate to roughly a 22.5 m decline in water elevation. Such a dramatic drop in water elevation does not compare well with the estimated 9 m drop, suggesting that glacier thinning has not had a significant role in outburst timing.

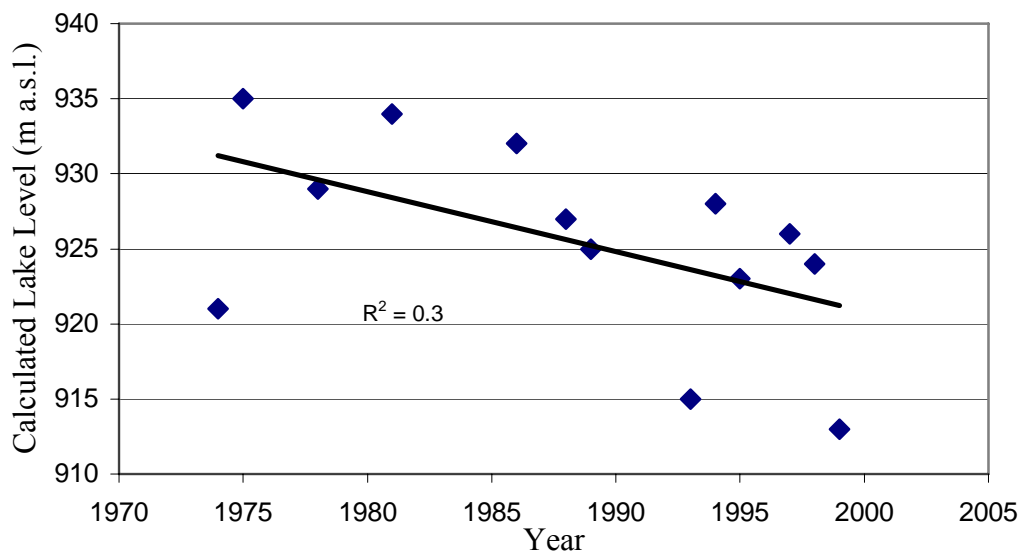


Figure 14. Plot of calculated lake level against time of outbreak for Hidden Creek Lake.

Location of the subglacial hydraulic system

Because Thorarinsson's and Nye's flotation and cantilever theories require the lake water to connect with a developed fast hydraulic system before drainage can occur, the location of the nearest branch of the hydraulic system relative to the lake should help control outbreak timing. For example, if the fast hydraulic system reaches the lake early in the season, drainage would occur earlier. Consequently, the year-to-year variations in the location of the fast hydraulic system relative to the ice dam could explain the poor correlation between water level and the time of outbreak. We hypothesize that the headward (up-glacier) development of the fast hydraulic system is linked to the up-glacier migration of the snowline (Nienow, 1994). The date when the snowline reaches the lake will vary from year to year depending on climatic variables. To infer the time that the hydraulic system reaches the lake, I calculated the position of the snowline on the glacier using the hydrologic model developed for estimating runoff.

To test whether the model could reasonably predict the location of the snowline, a qualitative analysis was performed by comparing the models predicted snowline elevation with the actual snowline elevation pictured in photos of the landscape adjacent to HCL. The photos used in this comparison consist of three oblique aerial images of the HCL basin, dated August 27, 1969, August 18, 1978, and August 31, 1984. The predicted snowline was calculated for each photo date by interpolating between the model's estimated snow depths at the midpoint of each elevation zone. Unlike in computing runoff, there was no correction applied to the model's prediction of snowline elevation. From this analysis, the model predicted the elevation of the snowline in the area of HCL to within an estimated ± 20 meters elevation. Because of this reasonably

good prediction, the model was used to estimate the day at which the snowline reached HCL for several known floods (Figure 15). Unsure of the affect that the ± 20 m error in predicted snow elevation may have on the timing of the snowline at the lake, a ± 5 day error was assumed. Although the correlation coefficient for the least-squares fit presented in Figure 15 is relatively low at -0.5 , it is significant at the 90% level. Based on this fit, there appears to be a correlation between the timing of outbreak to the location of the snowline. Furthermore, there appears to be a negative trend in the results that could explain the increasingly earlier outbreak times as presented in Figure 14. This suggests glacier thickness and lake elevation may not play a significant role in outbreak timing, and the increasingly earlier release date may simply be a function of the upglacier migration of the snow line from year to year. Clouding this conclusion, however, is the affect the ± 20 m error in predicting the snow elevation may have on the timing at which the snowline exceeded the lake, especially when considering the gentle slope of the glacier's surface.

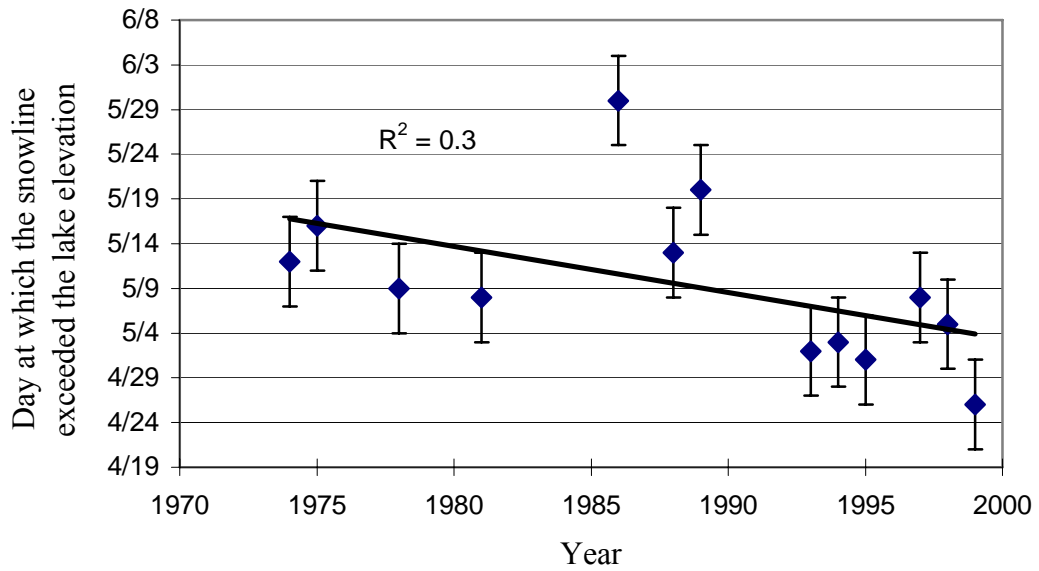


Figure 15. Plot comparing the location of the snowline to the time of outbreak.

Summary

The meteorological variables temperature and precipitation were evaluated individually using unique index systems to determine if a correlation between them and the time of outbreak exists. In addition, a lumped-parameter model was developed to gain insight into meteorological and hydrological properties that control runoff entering HCL. Although the model predicted runoff of the gaged basin of the Little Susitna River reasonably well, it remains uncertain how well the model predicts runoff entering HCL.

From these efforts, I conclude that:

- There is no direct relation between meteorological variables and the time of outbreak.

- There does not appear to be any correlation between lake level and the time of outbreak. This refutes Thorarinsson's (1939) and Nye's (1976) floatation and cantilever theories, respectively.
- There appears to be a declining trend in lake elevation with time. This decreasing trend could be the result of a reduction of ice dam thickness. However, evidence suggests that the ice dam thins much faster than the peak lake level drops.
- Lastly, it appears the location of the 'fast' hydraulic system correlates to the time of outbreak. Based on snowline information obtained from the hydrologic model, the time at which the 'fast' hydraulic system reaches the lake has decreased over the past few decades. This trend may help explain why there is a decline in lake elevation with time, since the closer the fast hydraulic system is to the lake, the less the ice dam is required to raise off the bed (hence, requiring less head in the lake) before a connection is made. Additional research is required to further evaluate the significance that snowline elevation has on correlating with the time of outbreak. Depending on the outcome, the location of the snowline may prove to be the best indicator of outbreak timing.

CHAPTER 4 - BOREHOLE WATER LEVEL ANALYSIS

Introduction

The most common method for accessing the subglacial hydraulic system is through boreholes. Because water levels in these boreholes provide a piezometric measure of basal water pressure (Hodge, 1974), glaciologists have been able to deduce the hydraulic properties of subglacial conditions. For example, under normal conditions the potentiometric surface is constant and maintains a water level in the borehole equal to roughly nine-tenths the ice thickness, equivalent to the ice-overburden pressure. Potentiometric measures that deviate from this condition suggest the presence of a subglacial hydraulic system. Fountain (1994) observed the potentiometric surface in boreholes to vary from levels matching ice-overburden pressure to levels well below the ice-overburden pressure. These levels also varied in time. Based on variations in basal water pressure, Fountain inferred that areas of low pressure correspond to regions near subglacial conduits. Others have observed similar water pressure variations, in addition to recording fluctuations in diurnal water-levels (Hubbard et al., 1995; Stone and Clarke, 1993; Iken et al., 1996). By analyzing how glacial hydraulic systems respond to these daily influxes, scientists have obtained valuable insight in understanding how some systems develop into an arborescent geometry (Shreve, 1972; Hooke, 1984). Moreover, hydraulic tests have also been performed in boreholes to provide a controlled measure of subglacial hydraulic properties (Stone and Clarke, 1993; Fountain, 1994; Hubbard et al, 1995; Waddington and Clarke, 1995;).

Due to the valuable information that can be obtained through boreholes established in glaciers, we had originally proposed to install an array of boreholes in the ice dam to evaluate how the hydraulic conditions changed in response to the outbreak. However, because of the early release time (only 3 days after we arrived on site), only one borehole was completed prior to outbreak.

Field Program and Methods

Based on earlier observations made by Rickman and Rosenkrans (1997), the lake drains through a subglacial system located on the south side of HCL. The drill site was therefore located south of the centerline of the ice dam, approximately 500 m east of the lake (Figure 16). The drill site was located far enough from the lake to assure that the ice was grounded and not part of the floating ice tongue. The specific site provided a relatively level working area and a water-filled crevasse – a critical source of water for drilling.

The drilling employed a high pressure hot water drill. The drill was borrowed from the University of Wyoming and was operated under the guidance of Dr. Joel Harper. A submersible water pump drew water from the crevasse and pumped it to a diesel-burning heater, where it was heated to approximately 82°C. The water was then pressurized by a high-pressure pump and routed through synflex hose to a weighted drill stem. The water exited the drill stem through a 4.8 mm diameter hole. The mass of the drill stem acted as a plumb bob and helped keep the borehole vertical. The hose was fed through a drill tower and downward progress of the drill stem was controlled by a

variable speed, gear driven motor mounted to the drill tower. During the drilling operations, the downward speed of the drill stem averaged about 1 m min.^{-1} .

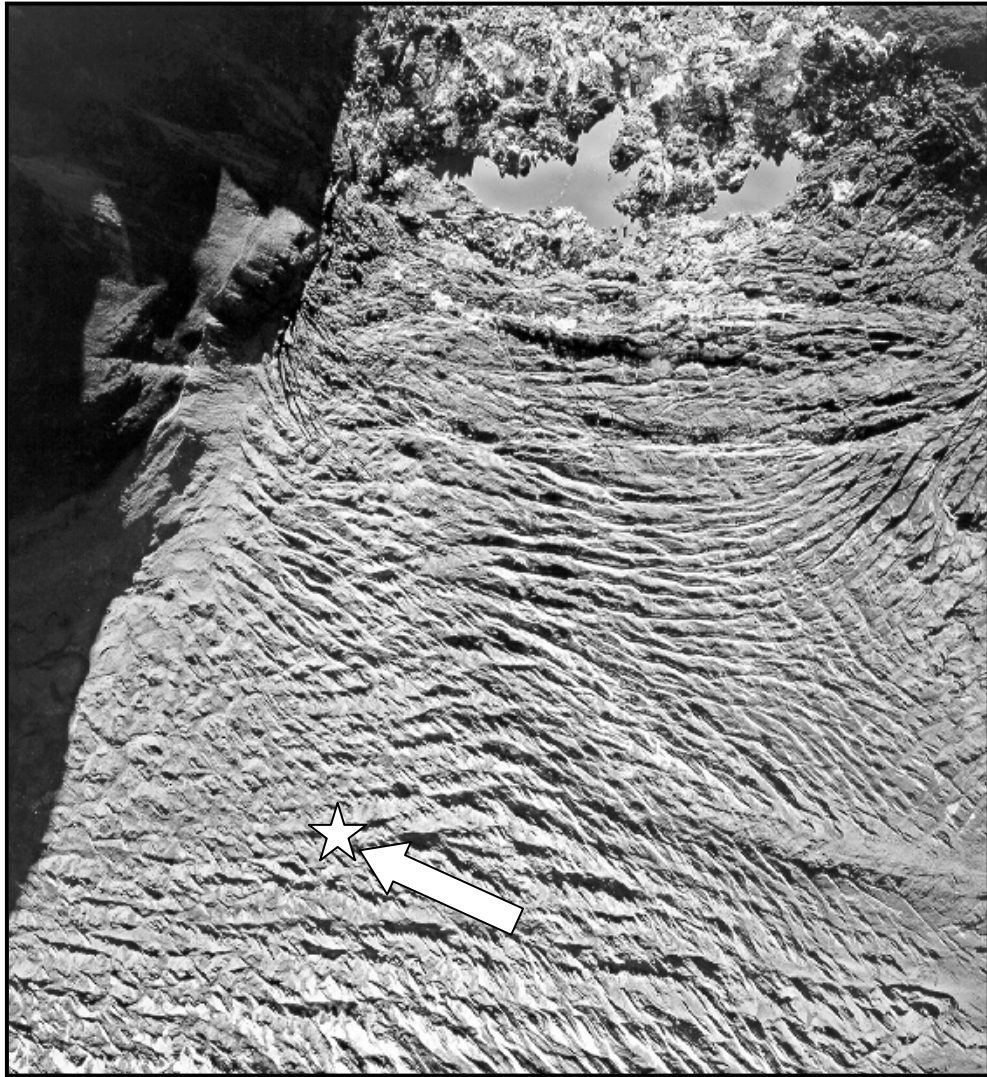


Figure 16. Aerial photo showing the location of the drill site (star) in relation to the lake (top of photo). For scale, the width of the ice dam is approximately 1 km wide. The top of the photo is to the west.

To determine the thickness of the glacier in the area of the drill site, an ice penetrating radar was operated by Mr. Andrew Malm of St. Olaf College, Minnesota. The results indicated a thickness of about 350 m. The coordinates of the drill site and radar transects were obtained via the use of a total station and were tied to the same datum established for the lake.

We drilled to a depth of 147 m before accumulated debris at the bottom of the borehole prevented further penetration. A borehole camera was lowered to identify the cause of the obstruction and to assess the nature of the borehole and the surrounding ice. It was not possible, however, to lower the camera to the bottom of the borehole. Based on a high proportion of debris observed within the ice walls of the borehole, it is presumed that englacial debris accumulated in the bottom of the hole as it was being drilled. At some point the weight of the debris could no longer be suspended by the jet of high pressure water from the drill and it finally clogged the hole, preventing further melt deepening.

To record the water level, 100 psi pressure transducers were lowered into the borehole and measurements were recorded every 10 minutes by a HOBO data logger (Onset Corp.). Based on calibration data provided by the manufacturer, the error of the pressure transducers was ± 0.06 m of water head. The water level measurements were referenced to the lake level by survey measurements previously described. During the outburst, the borehole water level dropped at a rate of several meters per hour, thus, corrections for atmospheric pressure were not necessary. The loggers also recorded air

temperature from sensors located within the data loggers with a manufacturer's estimated error of $\pm 1^{\circ}\text{C}$.

Chronology of events

July 15, 1999 (Julian Day 196): Drilling started in the morning. After drilling for several hours the water-level in the borehole dropped when the drill stem reached a depth of approximately 88 m below the ice surface (Figure 17). Drilling continued until late afternoon to a depth of 147 m, when drilling could no longer deepen the hole. The drill stem was removed and the water level was sounded using a float. The borehole water level was 22 m below the surface at 3:00 pm (15:00 hrs). A borehole camera was lowered down the borehole soon after and numerous rocks were observed in the hole at a depth of 54 m. The diameter of the largest rocks was about 2 cm. Based on the borehole video observations and on the estimated thickness of accumulated debris in the bottom of the borehole, I estimated that the glacier ice locally had a debris content of approximately 1% by volume. At 81 m below the surface, a stream of sediment pouring from an englacial feature was observed. After 30 minutes we reexamined the sediment discharge and it had apparently decreased. At 5:10 pm (17:10 hrs), the water level was recorded to have dropped to a depth of 29.3 m. At approximately 7:00 pm (19:00 hrs), news from Dr. J Walder indicated that the lake level was dropping.

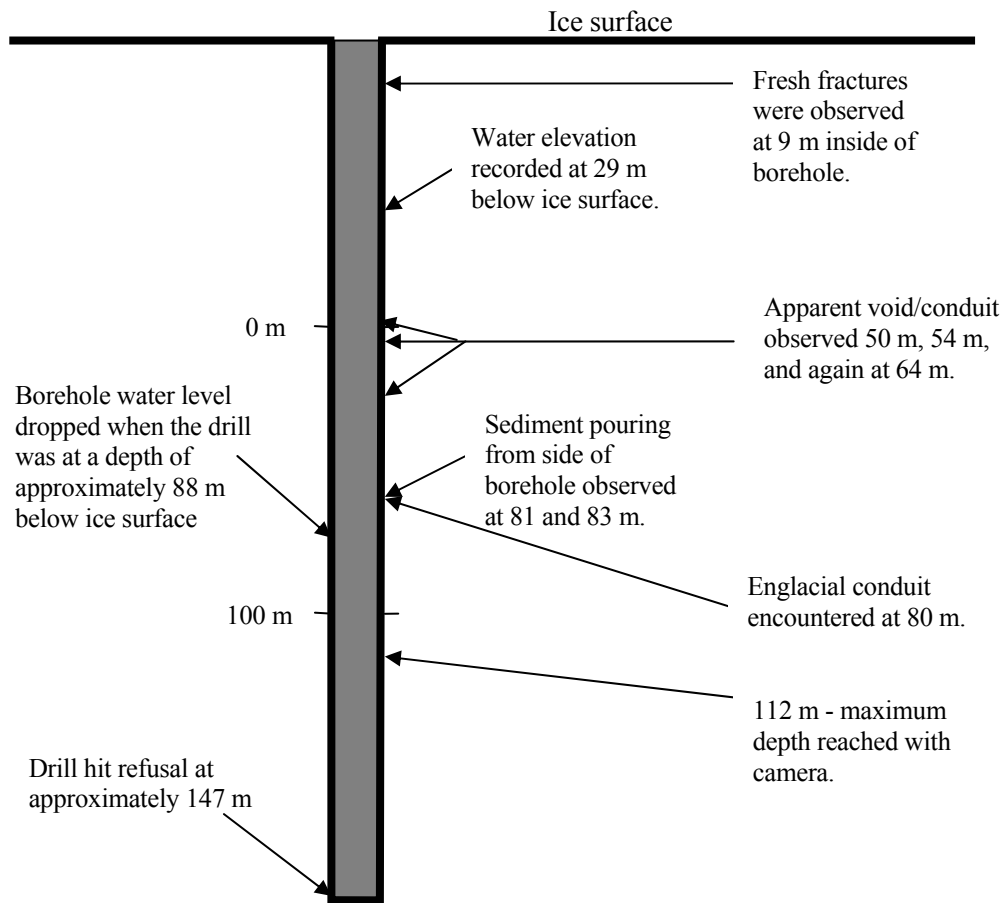


Figure 17. Diagram of borehole depicting the observations made during drill operations.

July 16, 1999 (Julian Day 197): At 12:00 am (00:00 hrs), the borehole was revisited and the depth to water was 31.6 m below the surface. At 1:09 am (1:09 hrs) the first transducer was installed at 72.6 m below the ice. At 3:20 pm (15:20 hrs), the borehole was again sounded using a float and the water level was 23.55 m. The transducer was checked and was found to be malfunctioning due to water leakage. At 10:43 pm (22:43 hrs) a significant amount of fracturing was heard at the drill site. At

this time the borehole was again sounded and the depth to water was 24.2 m. At 11:52 pm (23:52 hrs) a second transducer was installed to a depth of 70 m.

July 17, 1999 (Julian Day 198): The site was revisited at 12:15 pm (12:15 hrs) to confirm that the transducer was working properly.

July 18, 1999 (Julian Day 199): At 12:50 pm (12:50 hrs) numerous cracks were observed throughout the drill site (Figure 18), and the water-filled crevasse used for drilling had drained. Most of the water-filled crevasses in the area had also drained by this time. At 12:58 pm (12:58 hrs) the water had dropped below the level of the transducer. The borehole was then sounded to a depth of 97 m and no water was encountered. The transducer was pulled from the borehole

July 20, 1999 (Julian Day 201): The borehole camera was lowered down the dry hole. Fresh fractures in the side of the borehole were visible at 9 m (Figure 19). Several englacial voids or conduits were visible between 50 m and 64 m. At 80 m below the ice surface a conduit-like feature was observed. It was determined that this was the same feature that was observed having sediment pouring from it on July 16th (Figure 20). The camera was lowered to a maximum depth of 112 m and no standing water was encountered, despite observing water running down the side of the borehole.



Figure 18. Photo showing fresh fractures that propagated through the drill site. The width of the fractures is approximately 4-7cm.

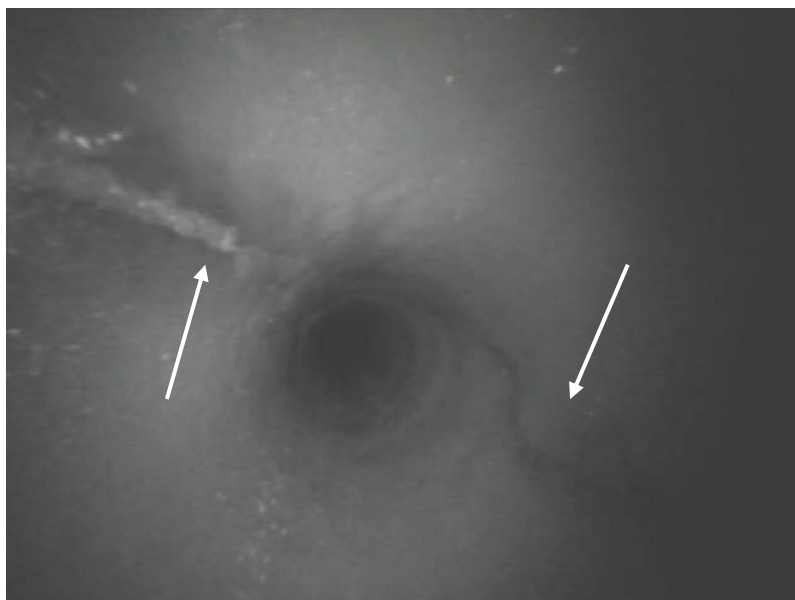


Figure 19. Fractures (arrows) observed within drained borehole on July 20, 1999. The photo is looking vertically down the borehole.

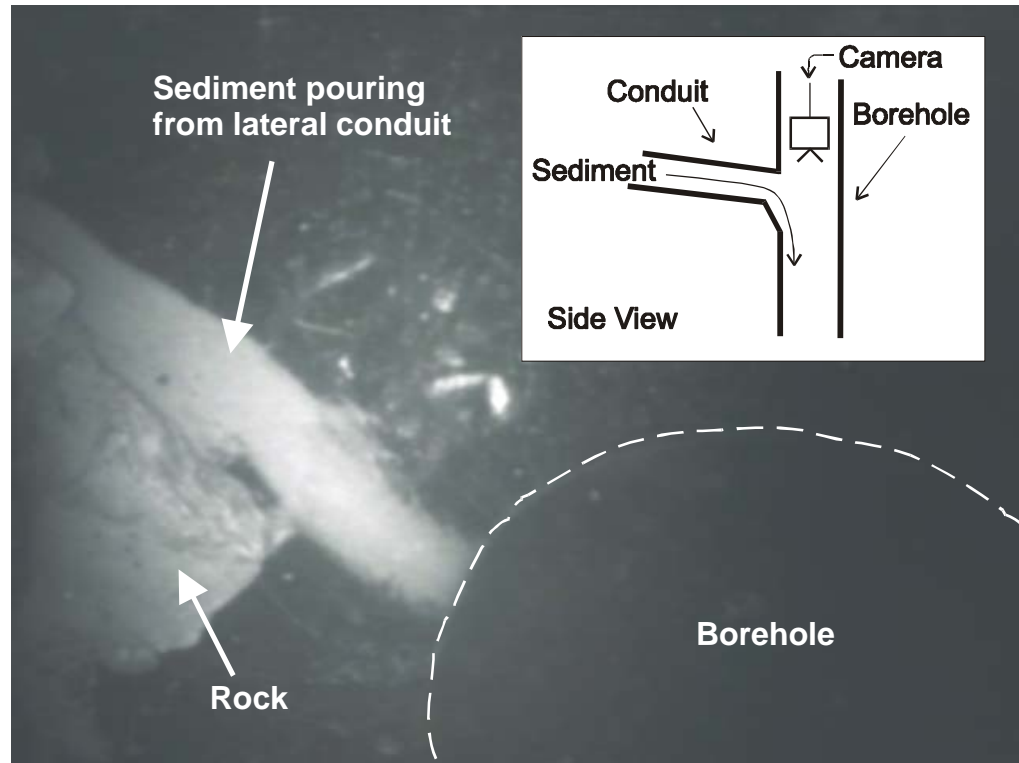


Figure 20. View of an englacial conduit with sediment pouring from it. The inset provides a cross-section view of the conduit geometry. The borehole, highlighted with a broken white line, is approximately 3-4 cm wide.

Results

Several gas filled pockets (voids) and an englacial conduit were observed in the borehole. The difference between voids and conduits is that voids are isolated and do not conduct water. Conduits, on the other hand, conduct water. In this study, the conduit was distinguished from voids by the presence of moving water, as evident by sediment flow. In addition, it was apparent when a void was encountered by the escape of pressurized gas and water at the glacier surface in the form of 3 - 4 m tall geysers.

Water levels obtained from the pressure transducers are presented in Figure 21a. The gap between the two sets of data represents the time period of transducer malfunction. Figure 21b presents the same set of water level data as in Figure 21a, but plotted with the lake water surface elevation. Two intriguing trends are of interest. The first, in Figure 21a, suggests a correlation between the air temperature and borehole water level during the afternoon of July 16. The second, in Figure 21b, indicates that on July 17 the falling borehole water level correlates with the lake level.

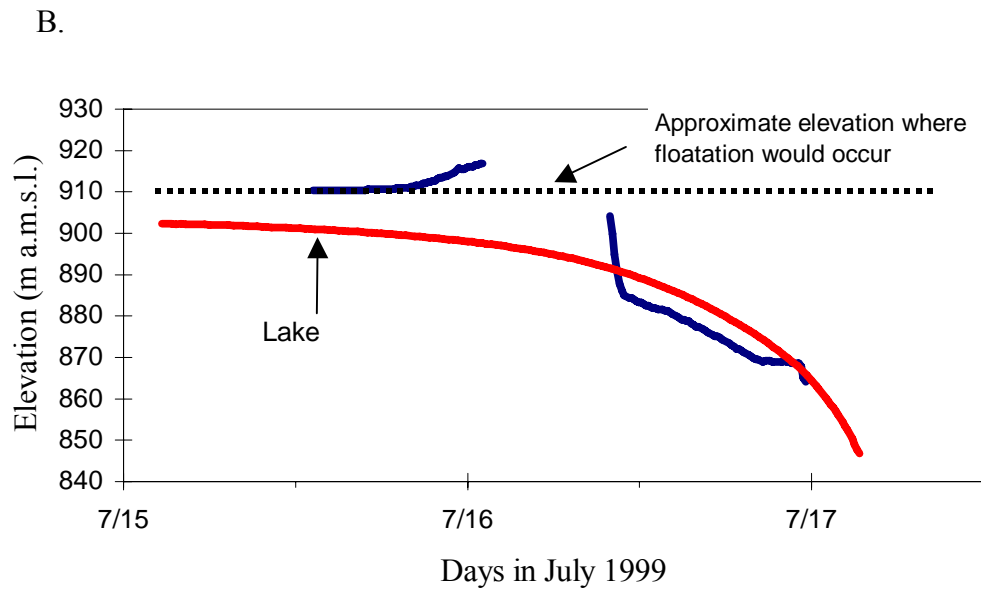
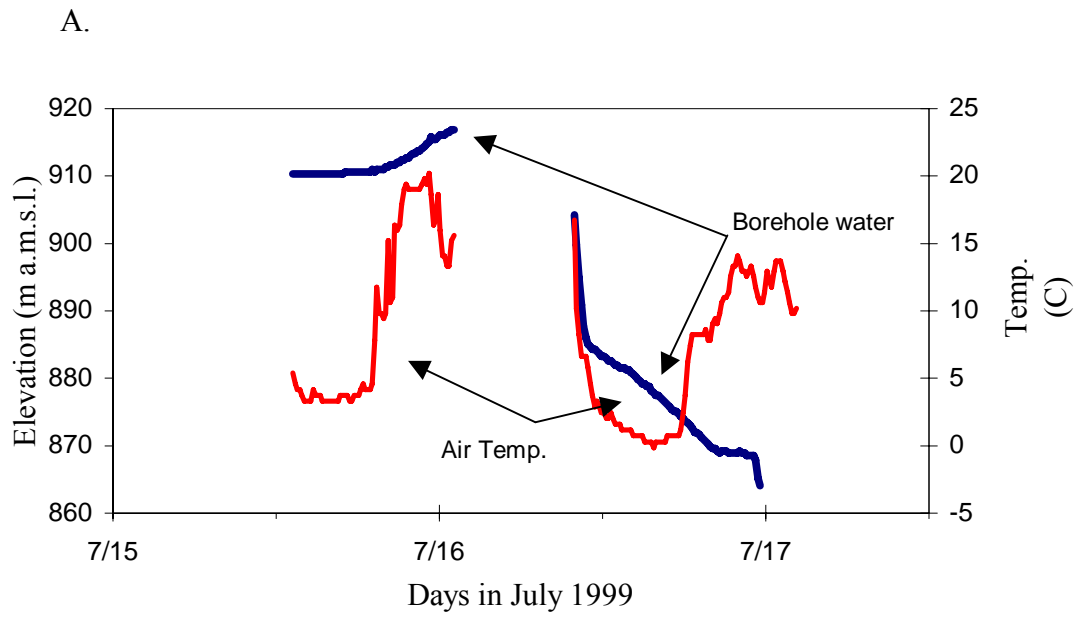


Figure 21. A) Plot of air temperature and borehole water level. B) Plot of lake and borehole water elevations.

Interpretation

The increase in borehole water level with increasing air temperature suggests that the borehole was connected to an englacial water system connected to the surface of the glacier. Warmer air temperatures cause more melt, which, after some lag time, reaches the englacial water system and are reflected as a rise in pressure. On July 16th the fractures heard propagating through the glacier, resulting from the ice dam lowering as lake level drops, created a direct connection between the lake and the borehole. In response, the water level in the borehole rapidly dropped until it reached equilibrium with the lake surface elevation. Just before the morning of July 17th, the rapid decrease in water level paused for a short time, before resuming again (Figure 22). This peculiar step-like feature is probably due to an influx of meltwater, note the rise in air temperature, temporarily compensating for the water lost during lake drainage. Continued cracking of the ice dam opened further passageways to the lake, which more than compensated for the increase in melt input, and the borehole water level again dropped to lake level. To determine whether this step is a result of melt influx (as opposed to some englacial hydraulic change), I compare this event to the first melt event previously described.

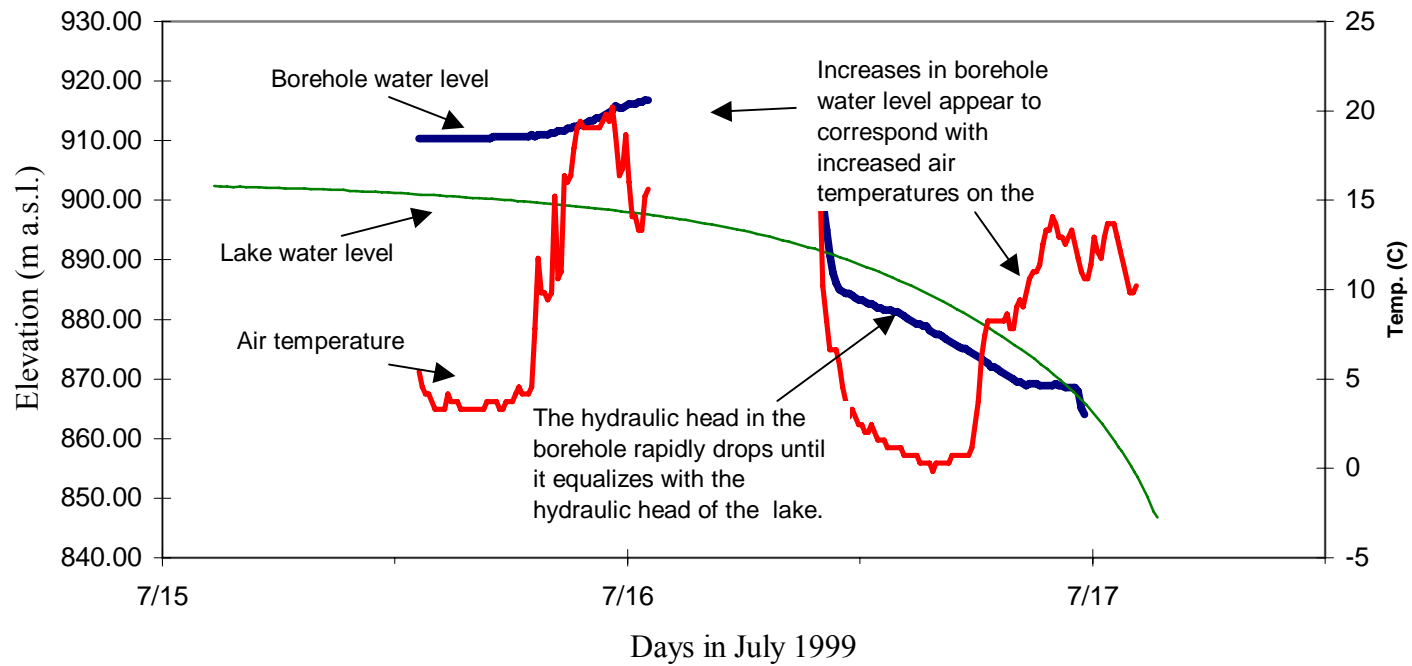


Figure 22. Illustrated plot of air temperature, and borehole and lake water elevations.

First, I infer the rate of inflow or outflow to the glacier interior from the slope of the borehole water level with time. Thus, positive slopes represent the net rate of inflow, and negative slopes represent the net rate of outflow. Based on this description, the borehole record was subdivided into three periods and piece-wise linear regressions were fitted to the data using a least squares fit (Figure 23).

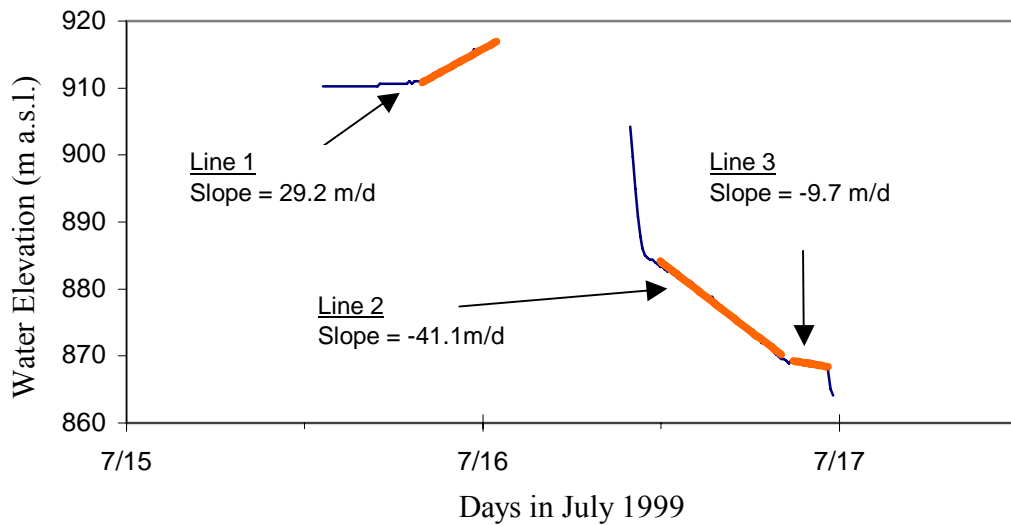


Figure 23. Illustrated plot showing the slope of portions of the borehole record.

Referring to Figure 23, Line 1 (29 m/d) probably reflects melt inflow going into the glacier. Line 2 (-41 m/d) is a fit of outflow due to the drop in HCL. During this time period, the ambient air temperature was near freezing (Figure 22) and very little surface melt was generated. As a result, the slope of Line 2 probably represents only the rate of outflow from the glacier. Line 3 (-9.7 m/d) may represent the water level change due to the difference in inflow from melt and outflow to the lake. Assuming for now that the melt inflow on July 16th (Line 1) is the same as the inflow on July 17th, and the rate of outflow during the early hours of July 17th (Line 2) is the same as later that day,

by summing inflow and outflow (slopes of Line 1 and Line 2) should result in a rate (slope) equivalent to Line 3. In performing this analysis, I am assuming that: 1) the drainage area influencing the surface inflow remains constant; 2) air temperature provides an adequate indicator of melt occurring on the glacier's surface; and, 3) the geometry of the borehole remains constant.

Inflow (Line 1) is 29 m day^{-1} , outflow (Line 2) is -41 m day^{-1} yielding a net difference of -12 m day^{-1} , close to the measured level change of -9.7 m day^{-1} in Line 3. The small difference between the calculated and measured rates may be due to different melt rates caused by differences in air temperature; the average temperature for July 16th was 9.7°C and the average temperature for July 17th was 3°C . After reducing the rate of inflow to reflect the decrease in temperature occurring on July 17th and recalculating outflow, we get a temperature-corrected water level change of -21.4 m/d . Although we can not completely account for the observed rate of outflow, it does appear that melt inflow is partly responsible for the unusual step-like feature represented by Line 3. Perhaps because of the severe cracking of the ice, assumption (1) or (3) may be invalid.

To assess whether or not the borehole water level matched the lake level drop during late July 16th and July 17th, the two records were directly compared. The data had been recorded at different time intervals, consequently, the lake data were converted to the same interval as the borehole data using linear interpolation procedure. A Lagrange polynomial provided the most accurate fit, as opposed to other interpolation methods, by performing a linear interpolation between each data point. After interpolation, the two data sets were subtracted and the difference plotted (Figure 24).

The difference in water levels was a near constant 6 m over the interval from 22:00 on July 16th to 09:00 on July 17th. The constant difference implies an efficient connection.

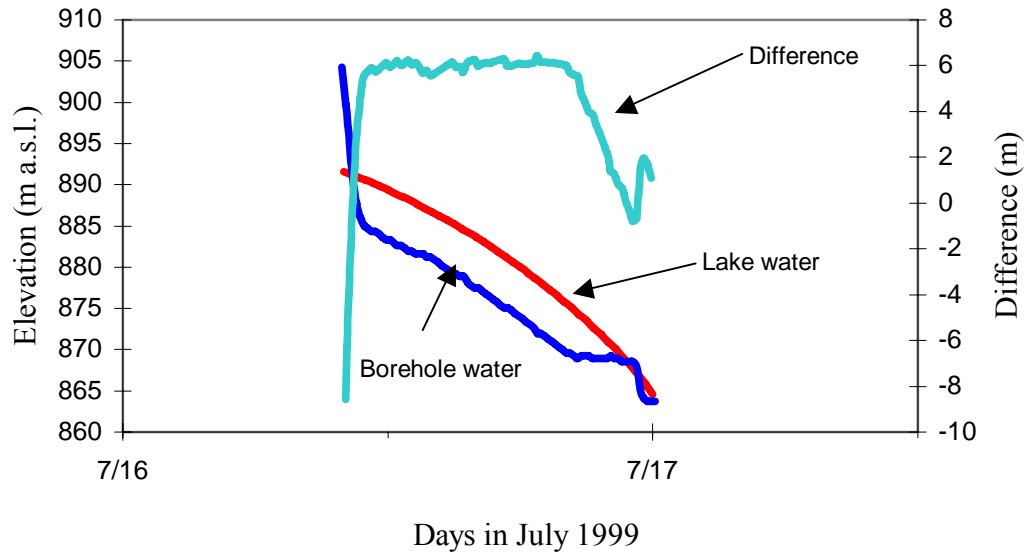


Figure 24. Plot comparing borehole and lake water elevations as the lake drained.

Summary and Discussion

The borehole water level record can be divided into two parts, the englacial record and the lake record. The first part of the record, from the start of data acquisition to noon on July 16th, indicates the pre-flood englacial condition and the second part of the record, after 7pm on July 16th, indicates the drainage of the englacial system during the flood. One unusual step-like feature in the borehole record, which could have been interpreted as the result of some internal hydraulic process, can be explained as an influx of surface melt water temporarily offsetting drainage. Starting on July 16th, the relatively constant and uniform 6 m change in borehole and lake water level suggests that the two systems were directly hydraulically connected. The difference in borehole

water response before and after flood initiation indicates the rapid evolution of the englacial hydraulic system from a moderately well connected system to a very well connected system. We presume the severe cracking in the ice dam opened new pathways for water flow to the lake.

The 6 m drop in head over the distance of 500 m from the lake to the borehole represents a hydraulic gradient of about 1%. By comparison, the difference in head between maximum lake level and the elevation at the terminus of the glacier is 488 m over 16.8 km, which equates to a gradient of about 3%. This low hydraulic gradient near the lake is probably due to the extreme crevassing and the vast number of water pathways. If the number of pathways were increased, the borehole water level would eventually equal the lake level. If the pathways were reduced, the gradient would probably match the overall gradient in the glacier. Alternatively, the flow path may be more sinuous than the estimated 16.8 km, resulting in a decreased gradient from the lake to the terminus of the glacier.

CHAPTER 5 – MODELING THE OUTFLOW HYDROGRAPH

Introduction

This chapter presents two mathematical models used for predicting flood discharge values for glacially-dammed lakes that drain subglacially. The first model is an empirical formula used to calculate peak discharge (Walder and Costa, 1996). The second model is a physically-based model that calculates the flood hydrograph as the lake drains (Clarke, 1982). The primary objective of this chapter is to compare the results of measured discharge values with values obtained by these mathematical models. By doing so, I hope to assess our theoretical understanding of outburst floods.

Comparison Data

In order to compare the modeled results to data from HCL, information on the discharge hydrograph exiting the lake and the peak discharge exiting at the terminus of the glacier was obtained.

In order to calculate the discharge hydrograph exiting the lake, changes in lake stage with time were recorded using a set of pressure transducers connected to data loggers. The positions of these transducers were tied into the same lake survey datum providing us with a recording of lake stage with time, dh/dt (Figure 10). By combining dh/dt with the storage curve (dV/dh), an exit hydrograph depicting the change in lake volume with time (dV/dt) was obtained (Figure 25). By integrating beneath the curve we get a maximum lake volume of approximately $16.6 \times 10^6 \text{ m}^3$.

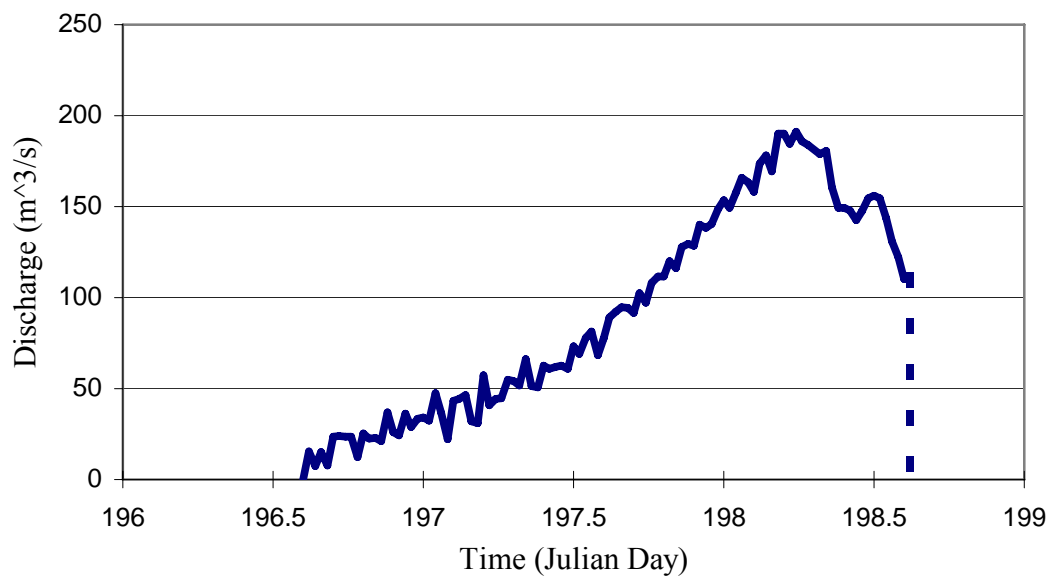


Figure 25. Plot of the flood hydrograph exiting Hidden Creek Lake. Assuming a vertical falling limb (dashed line) after the lake dropped below instrumented elevation.

The flood magnitude exiting the glacier was measured at the terminus in the Kennicott River by a team from the University of California, Santa Cruz (UCSC). By utilizing a footbridge that spans the Kennicott River at the terminus of the glacier, the team from UCSC installed stage recorders (sonic transducers) to continuously monitor river stage in a stilling well (Kraal, 2002). Periodic measurements of stream discharge were obtained by measuring the flow velocity and channel depth. The maximum discharge measured at the walking bridge, after subtracting out base flow, was approximately $204 \text{ m}^3 \text{ s}^{-1}$.

Walder and Costa Model

One of the first empirical formulas for estimating peak discharge of outburst floods is from Clague and Mathews (1973),

$$Q_{\max} = 75V_o^{0.67} \quad (r^2 = 0.96) \quad (7)$$

where Q_{\max} is the maximum discharge in $\text{m}^3 \text{s}^{-1}$ and V_o is the initial volume of the lake in 10^6 m^3 . Clague and Mathews developed this equation by fitting a regression line to 10 outburst floods of varying magnitudes and drainage types. The Clague and Mathews data set included both subglacial-drainage and breach-drainage floods. Since this equation was first published, more data have become available and similar models have been developed for different kinds of outburst floods, including earthen dams (Costa, 1988; Desloges et al., 1989; Walder and Costa, 1996). Of particular relevance is the work of Walder and Costa (1996) who revised equation (7) by separating the empirical data into subglacial-drainage and breach-drainage floods. For subglacial-drained floods, Walder and Costa (1996) expanded the dataset to include 26 of the most well characterized, subglacial-drained outburst floods, including the 1986 flood of HCL. Walder and Costa (1996) obtained the following relation for subglacially-drained floods:

$$Q_{\max} = 46V_o^{0.66} \quad (r^2 = 0.70) \quad (8)$$

Unlike equation (7), equation (8) defines a regression that fits several floods of only one type - subglacial outbursts. Consequently, equation (8) allows for a more

precise prediction and subsequent evaluation of peak discharge and downstream hazards posed by subglacial-drained outbursts.

I re-plotted the data from Walder and Costa (1996) and included the 1999 flood from HCL (Figure 26). Clearly, the HCL event is well within the range of outburst floods and there is no suggestion that it differs from the “typical” outburst flood. Using equation (8), the 1999 lake volume of $16.6 \times 10^6 \text{ m}^3$ yielded a peak discharge of $294 \text{ m}^3 \text{ s}^{-1}$, about $90 \text{ m}^3 \text{ s}^{-1}$ (45%) greater than the measured discharge of $204 \text{ m}^3 \text{ s}^{-1}$ exiting the terminus of the glacier. The prediction is arguably good considering the formula only depends on the initial volume of the lake, and requires no knowledge of key variables controlling discharge.

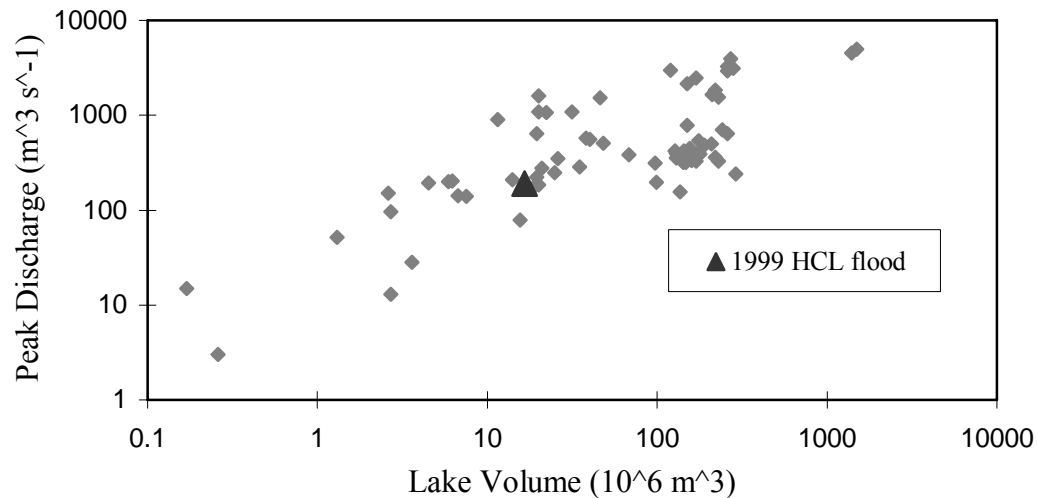


Figure 26. Plot showing the relation of lake volume to peak discharge, after Walder and Costa (1996). The black triangle is the 1999 HCL flood and the gray diamonds are floods from the Walder and Costa (1996) dataset.

Clarke Model

Following Nye's (1976) theoretical model of calculating the discharge hydrograph for the 1972 Grimsvötn flood, Clarke (1982) reworked Nye's model to include the geometry of the lake and retain the contribution of plastic creep to tunnel closure. Clark's model for calculating discharge (Q) is based on equations for tunnel geometry, continuity, energy conservation, and heat transfer, which are addressed in the following two coupled equations. For simplicity, the terms presented in the following are defined in Table 9.

$$\frac{dS}{dt} = \frac{S^{4/3} \langle -\partial\phi/\partial s \rangle^{3/2}}{\rho_l L N^{1/2}} + \frac{0.20 S^{2/3}}{\rho_l L'} \left(\frac{2\rho_w}{\eta} \right)^{4/5} \left(\frac{\langle -\partial\phi/\partial s \rangle}{\pi N} \right)^{2/5} k_w (\theta_{\text{Lake}} - \theta_i) - K_0 S \rho_l^n \left(1 - \frac{\rho_w h_w(t)}{\rho_l h} \right)^n \quad (9)$$

$$\frac{dV}{dt} = - \left(\frac{S^{4/3} \langle -\partial\phi/\partial s \rangle^{1/2}}{N^{1/2}} \right) \quad (10)$$

Equation (9) estimates the tunnel cross-section with time, where the first term on the right is the rate of tunnel enlargement by frictional heat derived from the release of potential energy, the second term is the rate of enlargement due to stored thermal energy in the lake water, and the third term represents the rate of closure by plastic creep.

Equation (10) represents the volume conservation in the lake with time.

Table 9. Model inputs

Inputs		Value	Units
Physical parameters			
Ice thickness at seal	h_i	300	m
Initial lake volume	V_o	16.6×10^6	m^3
Initial lake elevation above seal	h_o	270	m
Initial lake elevation above drainage tunnel outlet	$Z_w(0)$	481	m
Length of drainage tunnel	l_o	15000	m
Manning roughness coefficient	n'	0.105	$m^{-1/3}s$
Water influx to lake	Q_{in}	0	$m^3 s^{-1}$
Lake water temperature	θ_{lake}	1	C
Ice temperature	θ_i	0	C
Lake geometry	Hypsometric Curve (Figure 10)		
Physical constants			
Flow-law exponent	n	3	
Flow-law coefficient	B	2.16×10^{-24}	$Pa^{-3} s^{-1}$
Latent heat of fusion	L	333.5	$kJ kg^{-1}$
Specific heat capacity of water	c_w	4.217 7	$kJ kg^{-1} deg^{-1}$
Thermal conductivity of water	k_w	0.558	$W m^{-1} deg^{-1}$
Viscosity of water	η	1.787×10^{-3}	$kg m^{-1} s^{-1}$
Density of ice	ρ_i	900	$kg m^{-3}$
Density of water	ρ_w	1000	$kg m^{-3}$
Acceleration of gravity	g	9.8	$m s^{-2}$
Additional quantities and terms			
Constant defined by Nye (1976)	K	$= 2B3^{(n+1)^2}/n^n$	
Constant defined by Nye (1976)	N	$= (4\pi)^2/3\rho_w g n'^2$	$kg m^{-1} s^{-2}$
Effective latent heat of fusion for ice	L'	$= L$	$kJ kg^{-1}$
Ice pressure	p_i	$= \rho_i g h_i$	$kg m^{-1} s^{-2}$
Fluid potential gradient	$\langle -\partial\phi/\partial s \rangle$	$= \rho_w g_{zw}(t)/l_o$	$kg m^{-2} s^{-2}$

To simplify computation of equation (9) and (10), Clarke (1982) defined dimensionless variables for tunnel cross-section area $S^* = S/S_o$, time $t^* = t/t_o$, and discharge $Q^* = Q/Q_o$ where

$$S_o = \frac{V_o[\rho_w g Z_w(t)] / l_o}{\rho_i L'} \quad (11)$$

$$t_o = \frac{(\rho_i L')^{4/3} [(4\pi)^{2/3} \rho_w g n^2]^{1/2} l_o^{11/16}}{V^{1/3} [\rho_w g Z_w(t)]^{11/16}} \quad (12)$$

$$Q_o = \frac{V^{4/3} [\rho_w g Z_w(t)]^{11/6}}{l_o^{11/6} [(4\pi)^{2/3} \rho_w g n^2]^{1/2} (\rho_i L')^{4/3}} \quad (13)$$

Based on ice penetrating radar surveys performed by Mr. Malm of the bathymetry of the glacier in front of the lake, the seal to HCL is estimated to be about 300 feet below the top of the glacier, h_i , and about 270 m below the maximum lake elevation, h . Inputting these parameters and other parameters from Table 10 into equations 11, 12, and 13 gives $S_o = 17.38 \text{ m}^2$, $t_o = 139.60 \text{ hrs}$, and $Q_o = 33.02 \text{ m}^3 \text{ s}^{-1}$.

The final dimensionless quantities defined by Clarke (1982) include a “tunnel closure parameter” α (Equation 14), a “lake temperature parameter” β (Equation 15), and a “lake geometry parameter” M .

$$\alpha = \frac{(\rho_i L')^{4/3} [(4\pi)^{2/3} \rho_w g n^2]^{1/2} p_i^n K_o l_o^{11/6}}{V_o^{1/3} [\rho_w g Z_w(t)]^{11/6}} \quad (14)$$

$$\beta = 0.205 \left(\frac{\rho_i L'}{V_o} \right)^{2/3} \left(\frac{2\rho_w}{\pi^{1/2} \lambda} \right)^{4/5} \frac{[(4\pi)^{2/3} \rho_w g n^2]^{1/10} l_o^{53/30}}{[\rho_w g Z_w(t)]^{53/30}} k_w (\theta_{lake} - \theta_i) \quad (15)$$

The quantity α describes the relative importance of creep closure in controlling the rate of enlargement or closure of the tunnel. For $\alpha = 0$ there is no creep closure of the tunnel. The quantity β characterizes the relative importance of lake temperature in controlling the rate of enlargement of the tunnel due to the dissipation of thermal heat causing the tunnel walls to melt. For $\beta = 0$ the lake and ice temperature are identical and tunnel enlargement occurs by frictional heat alone. Lastly, M describes the reservoir geometry, and is equivalent to the slope of a first-order regression fit to the hypsometric data using least-squares. M can also be expressed simply as the ratio between the initial lake volume, V_o , over the product of the initial lake area, $A(h_o)$, and h_o (Clarke, 1982). For $M=1$ the reservoir has vertical walls, for $1/3 < M < 1$ the reservoir is bowl-shaped, and for $0 < M < 1/3$ the reservoir is horn-shaped. For HCL, substitution of the input parameters from Table 10 gives $\alpha = 13.5$, $\beta = 2.5$ at 1°C , and $M = 0.03$.

By defining the above dimensionless variables and quantities, Clarke re-writes equations (9) and (10) into two dimensionless, differential equations that express the change of tunnel cross-section area (S) near the seal and the change in lake volume (V) with time, respectively.

$$\frac{dS^*}{dt^*} = S^{*4/3} + \beta S^{*2/3} - \alpha S^* \left[1 - V^* (t^*)^M \right]^n \quad (16)$$

$$\frac{dV^*}{dt^*} = -S^{*4/3} \quad (17)$$

Equation (17) shows that discharge is proportional to tunnel cross-section area through simply $Q^* = S^{*4/3}$.

To explore the influences that creep closure, reservoir geometry, and lake temperature have on the magnitude of outbursts, Clarke used equations (16) and (17) to model the outburst of Hazard Lake, in the Yukon Territory, Canada. His results support Nye's (1976) conclusion and suggests that for a lake with $M < 0.5$ and $\alpha < 10^2$, the effect of creep closure is minor and does not change the outcome of the outburst flood hydrograph significantly. An example of this is presented in Clarke's Figure 5 (Clarke, 1982). Based on this outcome and the low values of α and M obtained for HCL, I elected to ignore creep closure and simplify the model.

By neglecting creep closure and setting $\alpha = 0$, the last term on the right-hand side of equation (17) disappears. Moreover, the effect of reservoir geometry (M) also disappears because M has a direct influence on regulating the effective pressure within the conduit by changing the hydraulic head. Thus, by neglecting creep closure, only lake temperature, β , needs to be considered. In the following, I examine the Hidden Creek Lake outburst without the effect of creep closure and explore how lake temperature, and other variables such as lake volume, channel length and roughness, and the ice thickness at the seal influence the outburst hydrograph. I attempt to compare the modeled hydrograph to measured results obtained from HCL. In these analyses equations (17) and (18) were solved simultaneously using a fourth-order Runge-Kutta algorithm.

Results

As indicated by Clarke (1982), the transfer of thermal energy from lake water has a significant effect on melt-enlargement of the conduit system. In theory, the warmer lake water, the more thermal heat transfer is available to melt-enlarge the conduit system, resulting in flood hydrographs that exhibit rapidly rising climbing limbs (short duration) with high peak discharges (high intensity). These short duration, high intensity hydrographs differ from the long duration, low intensity hydrographs that develop from lake water that is close to 0°C.

Friend (1988) reported water temperatures from HCL ranging from 0.16°C at a depth of 1.0 m to 1.81°C at a depth of 117 m. Temperature recordings at depths below 117 m were not measured. Because HCL is not isothermal at 0°C, hydrographs were computed for several different values of β ranging from 0.1°C to 4°C. As one would expect, changes in lake temperature have a significant effect in both the duration and peak discharge of the flood (Figure 27). By varying β for Hidden Creek Lake, the most reasonable fit to the flood hydrograph occurs when the lake waters are at 3°C ($\beta = 7.5$), and when the measured hydrograph is shifted ahead 40 hrs on the x-axis (Figure 28). This shift on the time axis is both reasonable and necessary in this numerical model because one cannot determine the initiation time from our measured data. With $\beta = 7.5$, the predicted discharge obtained using the Clarke model is 300 m³ s⁻¹, approximately 109 m³ s⁻¹ more than the measured peak discharge exiting the lake and 96 m³ s⁻¹ more than the measured peak discharge exiting at the terminus of the glacier. Interestingly,

the peak discharge obtained by the Clarke model differed by only $6 \text{ m}^3 \text{ s}^{-1}$ from the predicted peak discharge obtained using the Walder-Costa model.

This relatively good fit between the measured and modeled discharge values is misleading because, based on Friend's temperature sounding, it is unlikely that the average water temperature of Hidden Creek Lake is as warm as 3° C . Qualitatively averaging the water temperature per volume at each depth of the lake, the average lake temperature is about $1^\circ \pm 0.5^\circ \text{ C}$. Thus, it is assumed that errors in other input variables must be contributing to the reasonable fit with β calculated at 3° C . These errors may be imbedded in our measurement of lake volume, or in our estimate of the physical nature of the drainage system, such as the location of the seal and the length and roughness of the channel system. Alternatively, Clarke's model may be providing an unreasonable fit to the measured data due to variations in discharge caused by physical obstructions in the drainage system. The following addresses each of these issues.

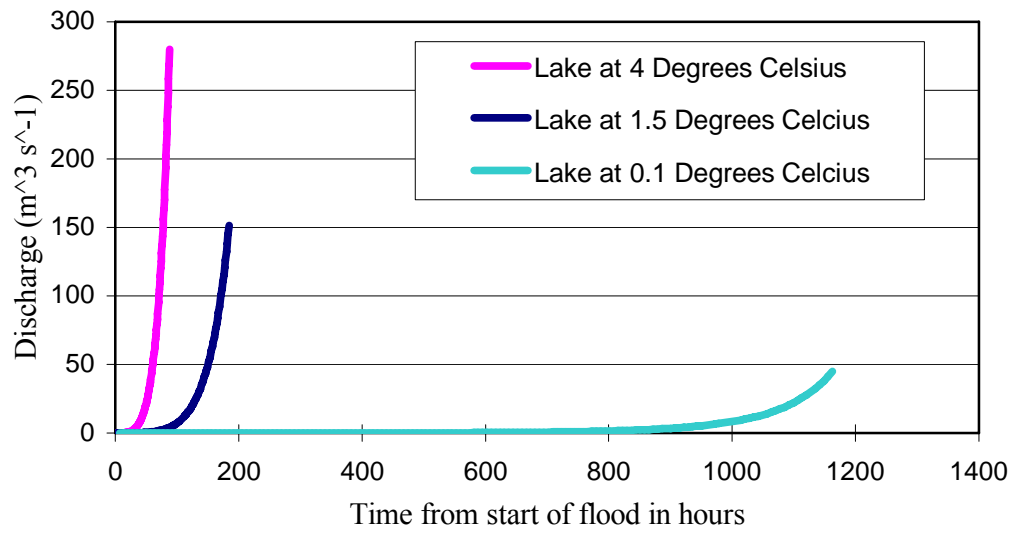


Figure 27. Predicted hydrographs using Clarke's 1982 solution. The point at which the graphs terminates is when the volume within the lake goes to zero.

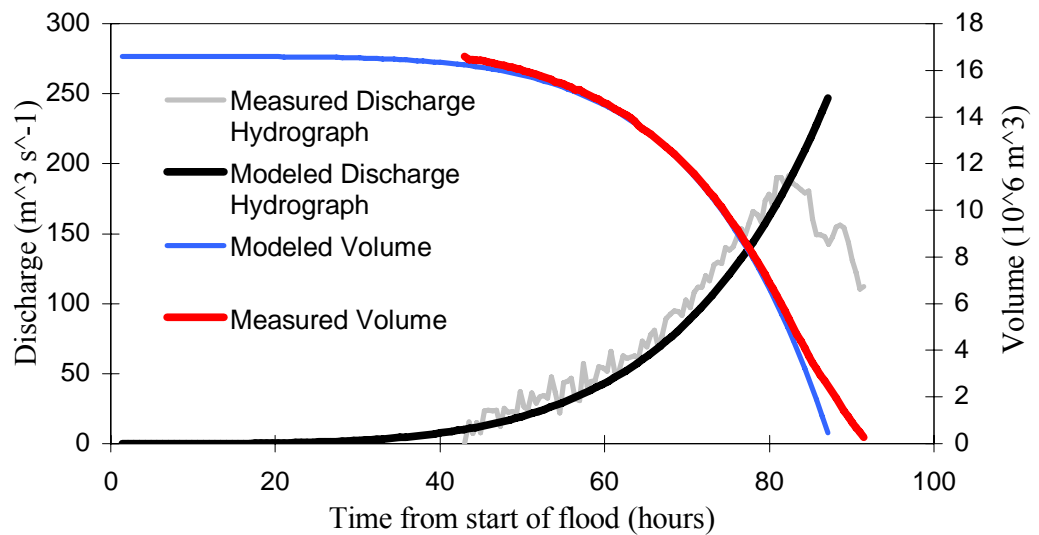


Figure 28. Plot comparing the modeled and measured hydrographs.

Lake Volume

Up to this point, the influence of floating ice within the lake and the volume of water located beneath the ice dam have been assumed to be equal and their influences have been ignored in the final volume calculation (Chapter 3). Although I am confident that this first order approximation of lake volume has not significantly affected earlier findings discussed herein, in Chapters 3 and 4, it may be influencing the Clarke model. Looking at equation (15), the dimensionless lake temperature parameter, β , in equation (17) is partially a function of the initial lake volume, V_0 . Consequently, if there were errors in our original measurements of lake volume, these errors would be propagated through the model and may be affecting the results.

Based on field observations and on aerial photos, 20% to 30% of the volume of the lake basin contained large icebergs after the lake had drained. However, correcting the final lake volume for the amount of water displaced by the ice is difficult; some of the ice may be grounded instead of floating. Whether these icebergs were present in the lake prior to the outburst or formed during the outburst is unknown.

Estimates of lake volume may also be influenced by the volume of water located beneath the floating ice dam. Efforts have been made to estimate this volume of water by using survey data at the glacier surface in the area of the floating dam and interpreting the bathymetry of the glacier beneath the ice dam (Cunico, 2002). The confidence of this volume estimate is speculative, however, and basing an analysis on it at this point would not be beneficial. Consequently, rather than attempting to quantify both the volume of water displaced by the icebergs and the volume of water beneath the floating dam, the Clarke model was re-evaluated with the lake temperature set at 1°C

and the original volume of $16.5 \times 10^6 \text{ m}^3$ was varied by $\pm 20\%$ (Figure 29). Although the lake volume was changed, the peak lake level was held constant since it did not change. The results indicate that a $\pm 20\%$ change in lake volume has little effect on the shape of the flood hydrograph but does alter the predicted peak discharge by increasing it by 18% from about $149 \text{ m}^3 \text{ s}^{-1}$ to $176 \text{ m}^3 \text{ s}^{-1}$ with the volume increase of 20% and by decreasing peak discharge about 25% from $149 \text{ m}^3 \text{ s}^{-1}$ to $119 \text{ m}^3 \text{ s}^{-1}$ with a volume decrease of 20%. This indicates that errors in estimates of lake volume are not exclusively responsible for the predicted hydrograph deviating from the measured hydrograph.

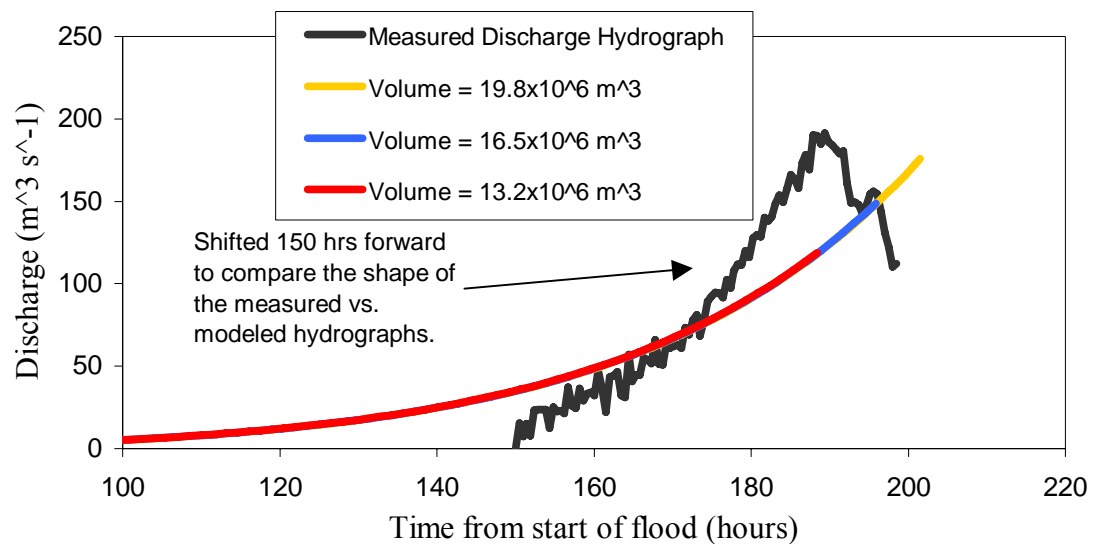


Figure 29. Comparison of modeled versus measured hydrographs where the lake temperature is held constant at 1 degree Celsius and lake volume varied by 20%.

Length of Drainage System

The channel was assumed to flow in a straight line from the lake to the terminus of the glacier with the exception of a slight bend in it, which is necessary to turn the corner from the lake out to the center of the glacier. This assumption may not be representative of the channel conditions, and may underestimate the length.

Lengthening the channel increases its sinuosity and decreases the hydraulic gradient (i.e., slope) of the channel system, resulting in a reduction in discharge. The effect of conduit length, l_o , was evaluated with l_o set at 15,000 m (a straight line) and 18,000 m (a 20% increase and sinuosity = 1.2). Results (Figure 30) show that increasing the length of the channel has little effect on changing the peak discharge. It does, however, significantly lengthen the duration of the flood.

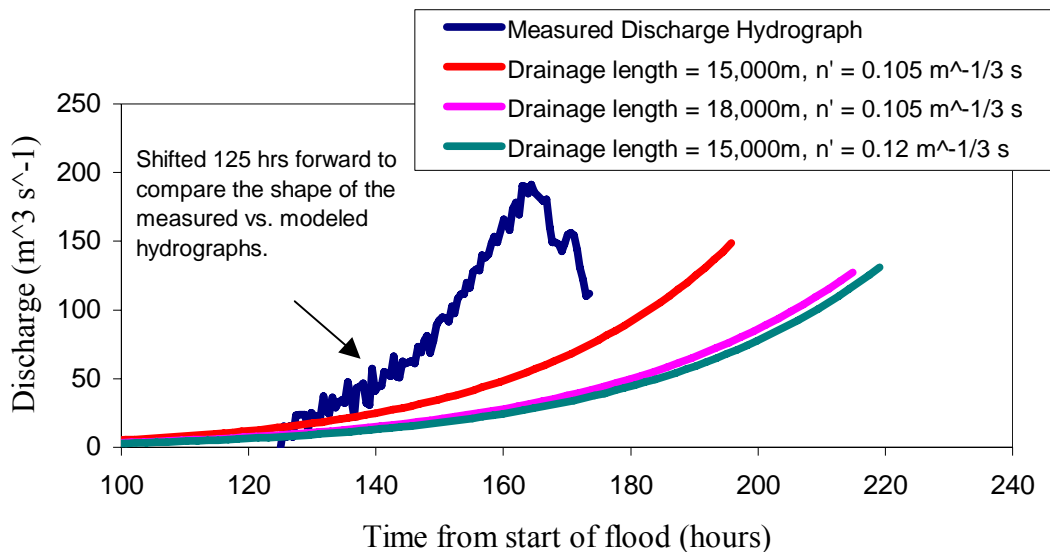


Figure 30. Plot comparing the measured hydrograph to modeled hydrographs with varying lengths and roughness.

Roughness of the Drainage System

The roughness of the channel, described by the Manning coefficient, is not well defined and has been a source of debate in the literature (Fountain and Walder, 1998). The rougher the channel surface, the slower the water moves through the system, resulting in greater friction and increasing melt enlargement. Initially, n' was $0.105 \text{ m}^{-1/3} \text{ s}$, equal to that used by Clarke (1982) for the Hazard Lake study. Nye (1972) used $0.12 \text{ m}^{-1/3} \text{ s}$ for the Grimsvötn flood. The result of varying n' from $0.105 \text{ m}^{-1/3} \text{ s}$ to 0.12 had a comparable effect as did increasing the length of the drainage system; it dramatically affected the flood hydrograph by increasing the necessary time to convey the floodwaters through the glacier but had only a small effect on the peak discharge by decreasing it by about $20 \text{ m}^3 \text{ s}^{-1}$ from $150 \text{ m}^3 \text{ s}^{-1}$ with $n' = 0.105 \text{ m}^{-1/3} \text{ s}$ to $130 \text{ m}^3 \text{ s}^{-1}$ with $n' = 0.12 \text{ m}^{-1/3} \text{ s}$ (Figure 30).

Initial Ice Thickness and Lake Elevation above Seal

The remaining parameters controlling the physical nature of the drainage system is the ice thickness located above the seal, h_i , and the initial lake elevation above the seal, h_o . Originally, the plan was to determine how these parameters affect the predicted discharge hydrograph. However, the solutions utilized in Clarke's (1982) analytical solution are not concerned with h_i or h_o because they are primarily functions of creep closure (Equation 14), which we have already determined to be insignificant for HCL. Thus, the influences of h_i and h_o were not evaluated.

Combination of Physical Parameters

Up to now, only the effects of independently altering individual parameters have been explored. However, it is natural to assume that errors within the individual parameters alone are not contributing to the poor fit between the modeled and measured hydrographs, but are rather a combination of errors that collectively prevent the two hydrographs from matching better. In this regard, different combinations of reasonable input parameters were computed to determine if an optimum combination of parameters could be obtained that would allow the modeled hydrograph to mimic that of the measured hydrograph. The results of this analysis indicate that the most accurate fit between the two hydrographs occurs when β is 8.43 with $V_o = 16.5 \times 10^6 \text{ m}^3$, $\theta = 3^\circ\text{C}$, $l_o = 16,000 \text{ m}$, $n' = 0.1 \text{ m}^{-1/3} \text{ s}$, and $Z_w = 481 \text{ m}$ (Figure 31). Out of all of these parameters, the value of θ equal to 3°C remains well above what is reasonable for HCL. Thus, there must be additional parameters that are not accounted for in Clarke's model. Examples of these parameters may include physical obstructions, as discussed in the following.

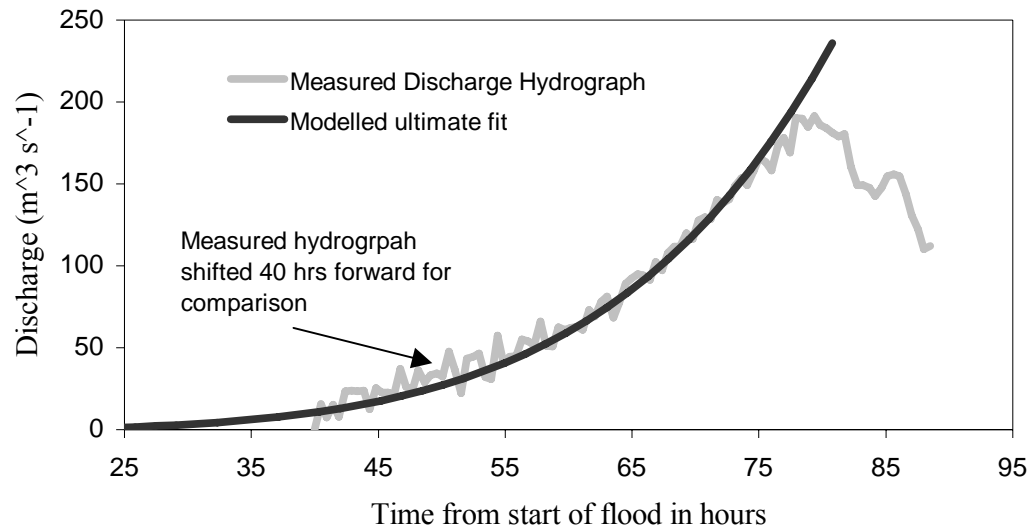


Figure 31. Plot comparing the measured hydrograph to a modeled hydrographs with the best combination of parameters where V_o is $16.5 \times 10^6 \text{ m}^3$, θ is 3°C , l_o is 16,000 m, n' is $0.1 \text{ m}^{-1/3} \text{ s}$, and Z_w is 481 m.

Speculation on Physical Obstructions

According to Nye (1976), the nominal flood hydrograph for subglacially released outbursts commonly has a long, exponentially increasing ascending leg that lasts for a few days, followed by a rapid drop. The reason for this exponential increase in discharge followed by a rapid drop is due to melt enlargement of the tunnel and emptying of the lake. The flood exiting Hidden Creek Lake, however, did not mimic the nominal flood as described by Nye (1976). The exit hydrograph for Hidden Creek Lake had an ascending leg similar to that expected for outburst floods, followed by a prolonged transition of varying discharge before assuming a rapid descending leg. Accordingly, hydrographs developed by the Clarke model resemble that of the nominal hydrograph and have peak discharges occurring at the moment when the last remaining

volume of water drains from the lake, the later of which is due largely to the fact that the solution ignores the function of creep closure. To illustrate the influence that creep closure has on the shape of the discharge hydrograph, the numerical solution of Clarke's model was explored with β set at 10, M set at 0.05, and α fluctuated. Results of this simulation indicate that only when $\alpha > 10^5$ does the hydrograph begin to take on a parabolic shape, with a gradual transition in discharge from increasing to decreasing. This is reflected in Clarke's (1982) Figure 5. From this analysis, one may be compelled to conclude that creep closure was a dominant factor toward the end of the flood and caused the anomalous parabolic shape of the measured discharge hydrograph. However, to numerically achieve this curve using the model requires a high ($\alpha > 10^5$) magnitude of creep closure. Such a value of creep closure is not physically possible at HCL. The question that still remains then is what mechanism might be responsible for the anomalous shape in the discharge hydrograph of HCL?

To offer a solution to this question, it is possible that some sort of obstruction occurred in the drainage system that caused the discharge to wane. In a study completed on the 1984 outburst flood of Strandline Lake, Alaska, Sturm et al. (1987) recorded five distinct episodes where discharge was abruptly reduced for short periods of time, all the while superimposed on an overall trend in which discharge was increasing nearly exponentially. They interpreted these reductions in discharge to be the result of a blockage or collapse within the subglacial tunnel system. They also reported that the 1986 flood of Strandline Lake was prematurely terminated, leaving the lake partially full. Based on these observations, it is hypothesized that some kind of obstruction

within the drainage system occurred and reduced the discharge from Hidden Creek Lake. This obstruction may be a large piece of ice calving from the glacier and getting lodged in the drainage system, or a collapse of a portion of the drainage system, possibly due to a rapid shift within the glacier.

CHAPTER 6 – DISCUSSION AND CONCLUSIONS

Summary

The primary objective of this research project was to elucidate the mechanisms responsible for the subglacial release of a glacially-impounded lake. In order to meet this objective, three subsidiary studies were conducted. First, a hydrologic model was constructed and information from it was used to correlate the time of outbreak with meteorological and physical factors. Second, a borehole was drilled in the glacier and water level data was analyzed to investigate how the englacial hydrology reacted in response to the flood. Last, the flood discharge was modeled using the empirical formula presented by Walder and Costa (1996) and by the numerical solution presented by Clarke (1982). The modeled discharge results were then compared to measured results and discrepancies between the two were analyzed.

Hypothesis 1: The timing of outbreak correlates with meteorological variables such as temperature and precipitation, changes in ice-dam thickness, or to the development of “fast” subglacial hydraulic systems that allow the water to drain.

After correlating the meteorological data with the outbreak date for 13 flood events, this research determined that air temperature and/or precipitation are not a good predictor of outbreak timing. Moreover, the flotation of the ice dam, as examined by the hydraulic head in the lake and the thinning of the glacier, could not be correlated with the time of outbreak. However, a general trend of decreasing lake head at the time of outbreak suggests that the glacier is thinning with time and perhaps provides an overall

control on outbreak timing. Arguably, the most important finding within this study is the determination that a possible correlation exists between the time of outbreak and the location of the snowline on the glacier. Using the snowline as an indicator of the up-glacier development of the ‘fast’ hydraulic system, it appears that the location of the ‘fast’ hydraulic system plays a significant role in controlling the time of release. This relationship is compelling, and suggests that a simple evaluation of the snowline may provide a means to predict the timing of outburst release.

Hypothesis 2: The englacial hydraulic system coincides with the hydraulic conditions of the lake, and the two systems act congruently through flood development.

A comparison of lake stage with the potentiometric surface within a borehole established in the glacier revealed that a connection between the englacial hydraulic system and the lake was established during outbreak; thus, allowing the two water surfaces to react congruently. From this relationship, it was hypothesized that surface melt entering the drainage system occurred, causing the discharge within the borehole to wane.

Hypothesis 3: Mathematical models allow us to predict how the floodwaters propagate through the glacier.

Large discrepancies were found between the modeled and the measured discharge values. Compared to measured values, both the Clarke (1982) and the Walder and Costa (1996) models over-predicted peak discharge for HCL. However, because the predicted discharge of the two models agreed with each other, and because the shape of

the outflow hydrograph deviated from the “nominal” outflow hydrograph, it is speculated that a constriction within the drainage system likely caused the predicted values to differ from the measured values. This constriction might be caused by the mechanical failure of ice around the tunnel under the ice dam, which resulted in the lake discharge fluctuating uncharacteristically for approximately 12 hours before rapidly dropping. Consequently, the measured flood hydrograph deviated from the nominal flood hydrograph in that it did not have an exponentially rising limb followed by an abrupt and rapid falling limb.

Suggestions for future research

Although the hydrologic model used in this study predicted the discharge of the gaged Little Susitna River with an error of $\pm 21\%$, the accuracy of this model to predict the volume of water entering HCL could not be directly determined as there was no gaging of Hidden Creek. It is, therefore, recommended that future studies of HCL establish a gage station on Hidden Creek just before it flows into the lake. It would be advisable to install the gage station as early in the season as possible. Information from the gage system could be used directly in the determination of inflow entering the lake. Data from the gage could additionally be used to calibrate the hydrologic model. Once calibrated, the model could be used as a tool to study past floods, and as a predictive tool for future floods. Moreover, with the amount of inflow entering the lake known, a determination could be made on whether the dam leaks or not.

Assuming the snowline provides an indicator to the upglacial advancement of the “fast” hydrologic system, the model was used to estimate the location of the snowline on

the glacier and a correlation analysis between it and the timing of outbreak was performed. Results indicate that a compelling correlation between the location of the snowline and the timing of outbreak does exist. However, because the accuracy of the model to predict the level of snowline was difficult to ascertain, additional work is necessary to corroborate this finding. It is, therefore, suggested that more accurate surveys be performed on the glacier to monitor the location of the snowline through the season.

In this analysis only one borehole was drilled in the glacier before the flood ensued. In addition, this borehole did not reach the bed due to an accumulation of englacial debris. For future studies, it is recommended to arrive earlier in the summer (i.e., prior to July 1) to provide enough time to establish more boreholes. To overcome problems of accumulated debris in the borehole hindering the downward advancement of the drill stem, it is recommended to equip the drill stem with an angled tip. After lowering the drill stem to the bottom of the borehole, hot water is pumped through the drill stem and the angled tip melts out a large cavity on the side of the borehole. With some luck, debris will be washed into this cavity, allowing the borehole to again be advanced downward, after reinstalling a vertical tip.

In this research study we compared the volume of water stored in the lake with estimated volumes flowing into the lake and obtained a large discrepancy between the two. Although much of this discrepancy is likely the result of the inability of the simple hydrologic model to quantify the true volume of water entering the lake, some of the discrepancy could be attributed to errors in determining the basins hypsometry. To

better address this problem, future studies need to measure the lake hypsometry with more precise measurements than those utilized in this study. When the lake drains, the bottom of the lake becomes choked with large icebergs and, thus, does not allow the use of common survey techniques to measure the hypsometry; this includes using either a total station and prism or remote sensing methods such as laser altimetry or aerial photo interpretation. The only means of obtaining this data is to sound the bottom of the lake when it is full. This will involve using echo sounding or radar techniques. Once the hypsometry is known, the information could be used to calculate the water volume in the lake.

REFERENCES CITED

- Anderson, E.A., 1968, Development and Testing of Snow Pack Energy Balance Equations: *Water Resources Research*, v. 4, p. 19 - 37
- Anderson, E.A., 1973, National Weather Service Weather forecast system-Snow accumulation and ablation model. Silver Spring, Maryland: U.S. National Oceanic and Atmospheric Administration, NWS Technical Memorandum Hydro-17.
- Benn, D.I. and Evans, D.J.A., 1998, *Glaciers and Glaciation*: New York, Arnold Publishing Company, 734 p.
- Björnsson, H., 1974, Explanation of jökulhlaups from Grimvötn, Vatnajökull, Iceland: *Jökull*, v. 24, p. 1-26
- Björnsson, H., 1998, Hydrological characteristics of the drainage system beneath a surging glacier: *Nature*, v. 395, p. 771-774
- Boulton, G.S. and Hindmarsh, R.C.A., 1987, Sediment deformation beneath glaciers: rheology and sedimentological consequences: *Journal of Geophysical Research*, v. 92, p. 9059-9082
- Braithwaite, R.J., 1984, Calculation of degree-days for glacier-climate research: *Zeitschrift Für Gletscherkunde und Glacialgeologie*, v. 20, p. 1-8
- Clague, J.J., and W.H. Mathews, 1973, The magnitude of jökulhlaups: *Journal of Glaciology*, v. 12, p. 501-504
- Clarke, G.K.C., 1982, Glacier outburst floods from "Hazard Lake," Yukon Territory, and the problem of flood magnitude prediction: *Journal of Glaciology*, v. 28, p. 3-21
- Clarke, G.K.C., 1996, Lumped-element analysis of subglacial hydraulic circuits: *Journal of Geophysical Research*, v. 101, p. 17547-17559
- Collins, D., 1979, Quantitative determination of the subglacial hydrology of two alpine glaciers: *Journal of Glaciology*, v. 23, p. 347-362
- Costa, J. E., 1988, Floods from dam failures. In Baker, V.R., Kochel, R.G., and Patton, P.C. (eds), *Flood Geomorphology*. Wiley, New York, p. 439-463

- Cunico, Michelle, 2002, unpublished master's thesis
- Desloges, J.R., Jones, D.P. and Ricker, K.E., 1989, Estimates of peak discharge from the drainage of ice-dammed Ape Lake, British Columbia, Canada: *Journal of Glaciology*, v. 35, p. 349-354
- Donn, William (1951), *Meteorology*. McGraw-Hill Book Company, Inc., New York, p. 465
- Driedger, C.L., and Fountain, A.G., 1989, Glacier Outburst Floods at Mount Rainer, Washington State, U.S.A.: *Annals of Glaciology*, v. 13, p. 51-55
- Fischer, U.H., Iverson, N.R., Hanson, B., Hooke, R.L., and Jansson, P., 1998, Estimation of hydraulic properties of subglacial till from ploughmeter measurements: *Journal of Glaciology*, v. 44, p. 517-522
- Fountain, A.G., 1992, Subglacial water flow inferred from stream measurements at South Cascade Glacier, Washington State, U.S.A.: *Journal of Glaciology*, v. 13, p. 51-64
- Fountain, A.G., 1994, Borehole water-level variations and implications for the subglacial hydraulics of South Cascade Glacier, Washington State, U.S.A.: *Journal of Glaciology*, v. 40, p. 293-304
- Fountain, A.G. and Walder, J.S., 1998, Water flow through temperate glaciers: *Reviews of Geophysics*, v. 36, p. 299-328
- Fowler, A.C., 1999, Breaking the seal at Grimsvötn, Iceland: *Journal of Glaciology*, v. 43, p. 506-517
- Fowler, A. and Walder, J., 1993, Creep closure of channels in deforming subglacial till: *Proc. R. Soc. London, Ser.A*, v. 441, p. 17-31
- Friend, D.A., 1988, Glacial outburst floods of the Kennicott Glacier, Alaska --an Empirical Test [Master of Arts Thesis in Geography]: University of Colorado, Boulder, Colorado, 96 p.
- Gilbert, R., 1972, Drainage of Ice-dammed Summit Lake, British Columbia: Inland Waters Directorate, Water Resources Branch, Ottawa, Canada, Scientific Series No. 20, 17 p.
- Glen, J.W., 1954, The stability of ice-dammed lakes and other water-filled holes in glaciers: *Journal of Glaciology*, v. 2, p. 316-318

- Haeberli, W., 1983, Frequency and characteristics of glacier floods in the Swiss Alps: *Annals of Glaciology*, v. 4, p. 85-90
- Hallet, B. and Anderson, R.S., 1982, Detailed glacial geomorphology of a proglacial bedrock area at Castleguard Glacier, Alberta, Canada: *Glacialgeology*, v. 16, p. 171-184
- Harr, R.D., 1980, Some characteristics and consequences of snowmelt during rainfall in western Oregon: *Journal of Hydrology*, v. 53, p. 277-304
- Hock, R., 1999, A distributed temperature-index ice-and snowmelt model including potential direct solar radiation: *Journal of Glaciology*, v. 45, p. 101-111
- Hodge, S.M., 1974, Variations in the sliding of a temperate glacier: *Journal of Glaciology*, v. 13, p. 349-369
- Hooke, R. Le B., 1984, On the role of mechanical energy in maintaining subglacial water conduits at atmospheric pressure: *Journal of Glaciology*, v. 30, p. 180-187
- Hubbard, B.P., Sharp, M.J., Willis, I.C., Nielsen, M.K., and Smart, C.C., 1995, Borehole water-level variations and the structure of the subglacial hydrological system of Haut Glacier d'Arolla, Valais, Switzerland: *Journal of Glaciology*, v. 41, p. 572-583
- Humphrey, N., 1987, Basal hydrology of a surge-type glacier: observation and theory related to Variegated Glacier. Unpublished Ph.D. Thesis, University of Washington
- Iken, A., Fabri, K., and Funk, M., 1996, Water storage and subglacial drainage conditions inferred from borehole measurements on Gornergletscher, Valais, Switzerland: *Journal of Glaciology*, v. 42, p. 233-248
- Johnson, P.G., and Kasper, J.N., 1992, The development of an ice-dammed lake: The contemporary and older sedimentary record: *Arctic and Alpine Research*, v. 24, p. 304-313
- Kamb, B., 1987, Glacier surge mechanism based on linked cavity configuration of the basal water conduit system: *Journal of Geophysical Research*, v. 92, p. 9083-9100.
- Kasper, J.N. and Johnson, P.G., 1992, Drainage of an ice-dammed lake, Kaskawulch Glacier Basin, Yukon: *Northern Hydrology: Selected Perspectives*, p. 177-188

- Knight, P.G. and Tweed, F.S., 1991, Periodic drainage of ice-dammed lakes as a result of variations in glacier velocity: *Hydrological Processes*, v. 5, p. 175-184
- Knight, P.G. and Russell, A.J., 1993, Most recent observations of an ice-dammed lake at Russell Glacier, west Greenland, and a new hypothesis regarding the mechanisms of drainage initiation: *Journal of Glaciology*, v. 39, p. 701-703
- Kraal, E., 2002, unpublished research, University of California, Santa Cruz
- Lliboutry, L., 1983, Modifications to the theory of intraglacial waterways for the case of subglacial ones: *Journal of Glaciology*, v. 29, p. 216-226
- MacKevett, E.M., Jr., 1972, Geologic map of the McCarthy C-6 quadrangle, Alaska: U.S. Geological Survey Geologic Quadrangle Map GQ-979, scale 1:63,360.
- Marks, D. et. al., 1999, A spatially distributed energy balance snowmelt model for application in mountain basins: *Hydrological Processes*, v. 13, p. 1935-1959
- Melloh, R.A., 1999, A Synopsis and Comparison of Selected Snowmelt Algorithms: U.S. Army Corps of Engineers, Cold Regions Research and Engineering Laboratory, CRREL Report 99-8, 17 p.
- Nienow, P., 1994, Dye-tracer investigations of glacier hydrological systems, Ph.D. dissertation, Univ. of Cambridge, Cambridge, England
- Nolan, M., and Echelmeyer, K., 1999a, Seismic detection of transient changes beneath Black Rapids glacier, Alaska, U.S.A.: I. Techniques and observations: *Journal of Glaciology*, v. 45, p. 119-131
- Nolan, M., and Echelmeyer, K., 1999b, Seismic detection of transient changes beneath Black Rapids glacier, Alaska, U.S.A.: II. Basal morphology and process: *Journal of Glaciology*, v. 45, p. 132-146
- Nye, J.F., 1973, Water at the bed of a glacier, *in* symposium on the Hydrology of Glaciers, IAHS Publication, 94, p. 157-161
- Nye, J.F., 1976, Water flow in glaciers: jökulhlaups, tunnels and veins: *Journal of Glaciology*, v. 17, p. 181-207
- O'Connor, J.E. and Baker, V.R., 1992, Magnitudes and implications of peak discharges from glacial lake Missoula: *Geological Society of America Bulletin*, 104, p. 267-279

- Rana, B., Yoshihiro Fukushima, Yutaka Ageta, and Masayoshi Nakawo, 1996, Runoff modeling of a river basin with a debris-covered glacier in Langtang Valley, Nepal, Himalaya: *Bulletin of Glacier Research*, v. 14, p. 1-6
- Raymond, C.F., Benedict, R.J., Harrison, W.D., Echelmeyer, K.A., and Sturm, M., 1995, Hydrological discharges and motion of Fels and Black Rapids glaciers, Alaska, U.S.A.: implications for the structure of their drainage systems: *Journal of Glaciology*, v. 41, p. 290-304
- Röthlisberger, H., 1972, Water pressure in intra- and subglacial channels: *Journal of Glaciology*, v. 11, p. 177-203
- Richter, D.H., Rosenkrans, D.S., and Steigerwald, M.S., 1995, Guide to the Volcanoes of the Western Wrangell Mountains, Alaska – Wrangell-St. Elias National Park and Preserve: *U.S. Geological Survey Bulletin 2072*, 31 p.
- Rickman, R.L. and Rosenkrans, D.S., 1997, Hydrologic conditions and hazards in the Kennicott River basin, Wrangell-St. Elias national Park and Preserve, Alaska: *U.S. Geological Survey Water-Resource Inv. Rep. 96-4296*, 53 p.
- Seaberg, S.Z., Seaberg, J.L., Hooke, R. Le B. and Wiberg, D.W., 1988, Character of the englacial and subglacial drainage system in the lower part of the ablation area of Storglaciären, Sweden, as revealed by dye-trace studies: *Journal of Glaciology*, v.34, p. 217-227
- Sharpe, D.R., and Shaw, J., 1989, Erosion of bedrock by subglacial meltwater, Cantley, Quebec: *Geological Society of America Bulletin*, v. 101, p. 1011-1020
- Shreve, R.L., 1972, Movement of water in glaciers: *Journal of Glaciology*, v. 11, p. 205-214
- Stone, D.B. and Clarke, G.K.C., 1993, Estimation of subglacial hydraulic properties from induced changes in basal water pressure: a theoretical framework for borehole-response tests: *Journal of Glaciology*, v. 39, p. 327-340
- Stone, D.B., Clarke, G.K.C., and Ellis, R.G., 1997, Inversion of borehole-response test data for estimation of subglacial hydraulic properties: *Journal of Glaciology*, v. 43, p. 103-112
- Sturm, M., Beget, J., and Benson, C., 1987, Observations of Jökulhlaups from ice-dammed Strandline Lake, Alaska: implications for paleohydrology, in Mayer, L. and Nash, D., editors, *Catastrophic flooding, The Binghampton Symposia in Geomorphology, International Series 18*, Boston, MA, Allen and Unwin, p. 79-94

- Sturm, M. and Benson, C.S., 1985, A history of Jokulhlaups from Strandline Lake, Alaska, *Journal of Glaciology*, v. 11, p. 272-280
- Tangborn, W., 1980, Two models for estimating climate-glacier relationships in the North Cascades, Washington, U.S.A.: *Journal of Glaciology*, v. 25, p. 3-21
- Thorarinsson, S., 1939, The ice dammed lakes of Iceland with particular reference to their values as indicators of glacier oscillations: *Geografiska Annaler*, v. 21, p. 216-242
- Thorarinsson, S., 1953, Some New Aspects of the Grimsvötn Problem: *Journal of Glaciology*, v. 2, p. 267
- Tweed, F.S., and Russell, A.J., 1999, Controls on the formation and sudden drainage of glacier-impounded lakes: implications for jökulhlaup characteristics: *Progress in Physical Geography*, v. 23, p. 79-110
- U.S. Army Corps of Engineers, 1960, Engineering and Design-Runoff from Snowmelt: *Engineering Manual*, 1110-2-1406
- Waddington, B.S., and Clarke, G.K.C., 1995, Hydraulic properties of subglacial sediment determined from the mechanical response of water-filled borehole: *Journal of Glaciology*, v. 41, p. 112-124
- Waite, R.B., 1980, About forty last-glacial Lake Missoula jökulhlaups through southern Washington: *Journal of Glaciology*, v. 88, p. 653-679
- Walder, J.S., 1986, Hydraulics of subglacial cavities: *Journal of Glaciology*, v. 32, p. 439-445
- Walder, J.S., and Costa, J.E., 1996, Outburst floods from glacier-dammed lakes: The effect of mode of lake drainage on flood magnitude: *Earth Surface Processes and Landforms*, v. 21, p. 701-723
- Walder, J.S., and Driedger, C.L., 1995, Frequent outburst floods from South Tahoma Glacier, Mount Rainer, U.S.A.: relation to debris flows, meteorological origin and implications for subglacial hydrology: *Journal of Glaciology*, v. 41, p. 1-10
- Walder, J.S., and Fowler, A. 1994, Channelized subglacial drainage over a deformable bed: *Journal of Glaciology*, v. 40, p. 3-15
- Walder, J. and Hallet, B., 1979, Geometry of former subglacial water channels and cavities: *Journal of Glaciology*, v. 23, p. 335-346

Weertman, J., 1972, General theory of water flow at the base of a glacier or ice sheet:
Reviews of Geophysics and Space Physics, v. 10, p. 287-333